CATALINA M. RIVERA

DMRG ALGORITHM AND QUANTUM PHASE TRANSITIONS

DMRG ALGORITHM AND QUANTUM PHASE TRANSITIONS

CATALINA M. RIVERA

Master in Physics

Science

Professor: Andrés F. Reyes

July of 2013

To the memory of my father

1947 – 2010

ACKNOWLEDGMENTS

Agradezco a mi mamá por todo su amor y compañía incondicional, por aliviar mis cargas cuando mas lo necesitaba. A mi hermano por creer en mi, por sus consejos y sobre todo por alegrarme la vida. Al profesor Andrés F. Reyes por estos tres años de trabajo y aprendizaje constante, por su infinita paciencia para compartir conmigo su conocimiento y sus experiencias. A los profesores Alonso Botero y Luis Quiroga por su gran importancia en mi vida académica.

A mis amigos, en especial a Lau por su apoyo y por su muy valiosa colaboración en la realización de esta tesis, a Sergio por estar a mi lado y acompañarme en los momentos difíciles, a Shifo por sacarme de los pozos de la confusión, a Sebastián Montes por sus múltiples colaboraciones. A Albi, Migue, Yury, Nico, Pasto, Rudy e Ivan por su gran amistad y por ser parte de mi vida cotidiana.

CONTENTS

LIST OF FIGURES

LIST OF TABLES

1

INTRODUCTION

Many body problems are very difficult to solve since the Hilbert space dimension grows exponentially with the number of particles. A generic state in a Hilbert space of N particles can be expressed as:

$$|\psi\rangle = \sum_{i_1,i_2...i_N}^{d} C_{i_1,i_2...i_N}|i_1\rangle \otimes |i_2\rangle ... |i_N\rangle,$$

therefore we would need d^N coefficients to describe the state completely. One of the questions of major interest in physics is to figure out the ground state of many body systems. This lead us to the question of how does the phase diagram of a given system looks like.

The Numerical Renormalization Group method was developed by Kenneth Wilson in order to solve the impurity problem known as the Kondo model. The theoretical justification of NRG goes beyond the scope of this work and can be found in detail in [31]. In Chapter 2 we only announce the algorithm steps to develop NRG and follow [4] to implement it in the Bose Hubbard model. In this way we obtain the ground energy value as a function of the interacting parameter between the particles. In order to evaluate its performance we also had to compute the exact numerical solution as explained in [34], we present what we considered were the most interesting details of the computation that may be applied in other kind of problems.

Right after Wilson developed his NRG method to solve the Kondo problem, people tried to apply this method in order to study systems like the Hubbard and Heisenberg models in one dimension. Results were not very encouraging, since the method did not take into account the relations between the growing system and its environment. An alternative, based on varying the boundary conditions of the growing block, was suggested by White and Noack in 1992 [30] and turned out to be effective when studying single particle problems.

The other approach suggested also by White in [27] was based on entanglement properties of the system with its environment and is developed in terms of density matrices, the method is known as Density Matrix Renormalization Group DMRG. A first illustration of DMRG precision was given by White and Huse in 1993 [29], where the ground state of an antiferromagnetic chain with $S = 1$ was computed up to eleven orders of precision. Later in 2005 [21] among many other successful

calculations, the phase diagram of a one dimensional Bose Hubbard model was also calculated.

The efficiency of simulating a quantum many body system is based mostly on it's entanglement behavior. For example, if the entanglement of a subsystem with respect to the whole environment is bounded or grows at most logarithmically with its size, then it is possible to perform an efficient DMRG simulation. One dimensional ground states of spin chains [16] are known to satisfy this requirement. Despite the fact that in general higher dimensional systems are supposed to satisfy the area law for entanglement, DMRG applications to two dimensional systems have been made, see [5].

A direct way of using DMRG to study one dimensional systems is by analyzing the entanglement behavior of the first half of the chain. This is because the diagonalization of the reduced density matrix associated to the first half of the chain is part of the algorithm itself. In reference [9] the properties of the Schmidt gap (the difference between the first two higher eigenvalues of the reduced density matrix) have been studied for the transverse Ising model.

One of the main objectives of this work is to explain in detail the theoretical basis of the DMRG method and to give some important remarks that should be taken into account for those non expert readers interested in developing its own programming codes. This is done in Chapter 3 and in the Appendix.

In Chapter 4 we arrive to a very wide field of study in physics, Quantum Phase Transitions (QPT). We explore the idea of considering the Schmidt gap as an order parameter of the QPT present in the transverse Ising model, by performing the computations in other regions of the XY model.

Many other interesting ways of approaching QPT have been studied. We only mention here that recently a connection between the Berry Phase and QPT has emerged. In [35] it is shown that the geometric phase of the ground state for the XY model follows a scaling behavior and its derivative diverges at the critical point $\lambda_c = 1$. From a more topological point of view Chern numbers calculated for a certain geometric bundle associated to the ground state of the system can also serve to detect critical points and critical exponents as well. This has been done in [6] for the case of the XY model.

Furthermore there is a beautiful mathematical way of approaching the problem of QPT. This is done through the Gelfand- Naimark-Segal (GNS) construction. In [24] a theorem about how to know in this formalism if two states belong to the same 'physical world' or phase is given. We give a brief introduction to this topic in Chapter 5 in the spirit of establishing in future work a direct connection between this mathematical perspective and a more physical and numerical approach. In addition

we show the initial calculations done when we follow the formalism presented in [2] and apply it to the two site XY model with the final goal (out of the scope of this work) of generalizing it to the thermodynamic limit. In [2] a new way of approaching the problem of generalizing the notion of entanglement for fermionic and bosonic systems is proposed, the interesting fact being that the standard results for the entanglement are obtained as a particular case of the formalism.

A lot of work has to be done in the future to connect the different ideas presented in this project. We mention some potential avenues for future research in the last Chapter of Conclusions and Perspectives.

.....

2

NUMERICAL RENORMALIZATION GROUP

2.1 NUMERICAL RENORMALIZATION GROUP

The Numerical Renormalizaton Group NRG was developed by Wilson [31] in 1975 and is mainly used to approximate the ground state of one dimensional systems. The method deals with the problem of the exponential growing of the Hilbert space dimension as a function of the size of the system, by restricting it to a subspace generated by a truncated and rotated basis, so that the size of the system is increased while the dimension of the Hilbert space is kept constant at a value m.

The idea is to start with a small segment of the system and to enlarge it up to the desired size by discarding in each growing step the Hamiltonian eigenstates with the highest eigenvalues.

We will explain for now, the NRG method applied to spin chains. It is computationally convenient to start the algorithm with a small block of one or two sites described by a Hamiltonian term that we will denote H_B. For example, for a one-dimensional spin 1/2 quantum Ising model with a transverse magnetic field the initial block Hamiltonian for two sites would be $H_B = -J\,\sigma_1^z \otimes \sigma_2^z - h\,\sigma_1^x \otimes \mathbb{1}_2 - h\,\mathbb{1}_2 \otimes \sigma_2^x$, where J is the coupling constant and h the magnitude of the magnetic field. In general, we start an iteration with the H_B matrix of dimension $m_L \times m_L$, m_L representing the Hilbert space dimension of the system when it is composed of L sites; also, the $m_L \times m_L$ matrices σ_l^α and σ_r^α are needed, l and r representing the left and right sites of the block and $\alpha = x, y, z$ depending on the terms needed for constructing the interacting term. See Fig1

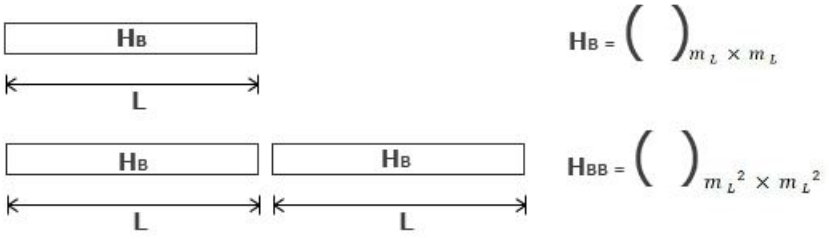

Figure 1

Then, we construct the Hamiltonian of two blocks joined together which we denote as $H_{BB} = H_{B_l} + H_{int} + H_{B_r}$, acting on a Hilbert space of dimension m_L^2. For creating the interacting term between the two blocks we need to use the matrices stored in the last step. In the example of the Ising model $H_{int} = -J\overline{\sigma}_r^z\overline{\sigma}_l^z$ with $\overline{\sigma}_r^z = \sigma_r^z \otimes 1_{m_L \times m_L}$ and $\overline{\sigma}_l^z = 1_{m_L \times m_L} \otimes \sigma_l^z$, also $H_{B_l} = H_B \otimes 1_{m_L \times m_L}$ and $H_{B_r} = 1_{m_L \times m_L} \otimes H_B$.

Figure 2

The next step is to diagonalize the Hamiltonian H_{BB}. In computational terms for the purpose of finding the ground state of the system it is only necessary to obtain the first $m_{2L} = \min(m_L^2, m)$ eigenstates, $\{|u_\nu\rangle\}$, $\nu = 1, 2, ..., m_{2L}$ (for example through the eigs function in matlab) corresponding to the highest eigenvalues. In this way we can perform the truncated change of basis through a matrix $T_{L\to 2L}$ of dimension $m_L^2 \times m_{2L}$ whose columns are the selected m_{2L} eigenstates. We finally project the Hamiltonian H_{BB} and the operators needed in the interaction term in this subspace and create the new block operators that will be used for the next iteration: $H_B = T^\dagger H_{BB} T$, $\sigma_\alpha^R = T^\dagger \sigma_\alpha^R T$ and $\sigma_\alpha^L = T^\dagger \sigma_\alpha^L T$. We have now, the same initial conditions to start a new iteration. Figure 3 shows an overall sketch of the algorithm just described.

Figure 3

2.2 NRG APPLIED TO THE BOSE HUBBARD MODEL

The Bose Hubbard model is an approximation used to describe interacting bosons in a lattice. Ultracold atoms in an optical lattice are often described with this model.

The Hamiltonian for a one-dimensional Bose Hubbard model with $N \equiv \sum_{i=1}^{I} n_i$ atoms in a lattice of length I is:

$$\hat{H} = -J \sum_{i=1}^{I-1} \{\hat{a}_i^\dagger \hat{a}_{i+1} + \hat{a}_{i+1}^\dagger \hat{a}_i\} + \frac{U}{2} \sum_{i=1}^{I-1} \hat{n}_i(\hat{n}_i - 1). \tag{2.1}$$

The operators $\hat{a}_j^\dagger$ and $\hat{a}_j$ are the creation and annihilation operators of a particle at site i and satisfy the commutation relations:

$$\begin{aligned} &[\hat{a}_i, \hat{a}_j] = 0 \\ &[\hat{a}_i^\dagger, \hat{a}_j^\dagger] = 0; \\ &[\hat{a}_i, \hat{a}_j^\dagger] = \delta_{ij} \end{aligned} \tag{2.2}$$

Also, the following expressions are satisfied:

$$\begin{aligned} \hat{a}_i \quad & |n_1, n_2, ..., n_i, ..., n_I\rangle = \sqrt{n_i} \quad |n_1, n_2, ..., n_i - 1, ..., n_I\rangle, \\ \hat{a}_i^\dagger \quad & |n_1, n_2, ..., n_i, ..., n_I\rangle = \sqrt{n_i + 1} \quad |n_1, n_2, ..., n_i + 1, ..., n_I\rangle, \end{aligned} \tag{2.3}$$

where $|n_1, n_2, ..., n_i, ..., n_I\rangle$ are states symmetric under spacial permutation of bosons with $N \equiv \sum_{i=1}^{I} n_i$ total particles, n_i located in site i. Consequently, $\hat{n}_i = \hat{a}_i^\dagger \hat{a}_i$ counts the particle number on that site:

$$\hat{a}_i^\dagger \hat{a}_i \quad |n_1, n_2, ..., n_i, ..., n_I\rangle = n_i \quad |n_1, n_2, ..., n_i, ..., n_I\rangle. \tag{2.4}$$

The first term in the Hamiltonian Eq.2.1 represents the kinetic part H_{kin}, where J describes the hopping probability of a particle between adjacent sites. The second term H_{int} represents the particle-particle interaction, where U is the interacting parameter. The expression $\frac{\hat{n}_i(\hat{n}_i - 1)}{2}$ counts the amount of interacting pairs that can be formed in a lattice site containing n_i atoms.

The dimension of the Hilbert space grows rapidly as a function of the lattice sites I and the number of particles N in the system; to be more precise this dimension is given by the following expression:

$$D = \frac{(N + I - 1)!}{N!(I - 1)!}. \tag{2.5}$$

A beautiful way to think about this formula is as follows: The basis vectors of the Hilbert space are vectors $|n_1, n_2, ..., n_I\rangle$ with the restriction $N \equiv \sum_{i=1}^{I} n_i$, the problem is simplified by the graphical representation in Fig 4, where we ask for the number of ways in which the $I-1$ black divisions can be moved to left or right increasing or decreasing the number of particles in each box. Since the black divisions are indistinguishable between them as well as the particles, we only need to calculate the number of ways in which $N+(I-1)$ objects can be organized when it is the case that there are only two kind of objects, N of the first type and $I-1$ of the second; as a result we obtain Eq.2.5.

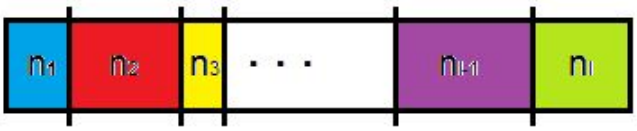

Figure 4

In Table 1 we present the Hilbert space dimension for some systems with $N = I$.

$I = N$	$\dim(H)$
3	10
6	462
8	6435
10	92378
11	352716
12	1352078

Table 1: Hilbert space dimensions for systems with $I = N$

2.2.1 *The ground state:*

Let us consider the ground states of the Bose Hubbard model in the two limiting situations of the parameter U/J: [4] For the case in which the interaction between the particles vanishes $U/J \ll 1$ the Hamiltonian reduces to the kinetic term which

tends to spread the single particle wave functions over the whole lattice. The system, then, is in the superfluid state and has the form:

$$|\psi_{SF}\rangle \propto (\sum_i \hat{a}_i^\dagger)^N |0...0\rangle. \tag{2.6}$$

On the other hand, when $U \gg J$, the interaction term is dominant in the Hamiltonian and tunneling is almost completely suppressed, consequently the system is in the Mott insulator state. In this state the single particle wave functions are localized at the lattice sites, and has the form:

$$|\psi_{MI}\rangle \propto \prod_i \hat{a}_i^\dagger |0...0\rangle. \tag{2.7}$$

2.2.2 *Results*

In Fig 5 we compare the results obtained using the NRG method with different initial range of particle numbers (NBlockMax= 8, 3) and the exact numerical solution to calculate the ground state of the Bose Hubbard model for $N = I = 8$ depending on the value of the parameter U/J. In Fig 6 the same results are shown but for the case of $N = I = 10$ and a range of particles given by (NBlockMax= 8, 10). In Appendices 1 and 2 we give computational details about the codes used to generate these graphics.

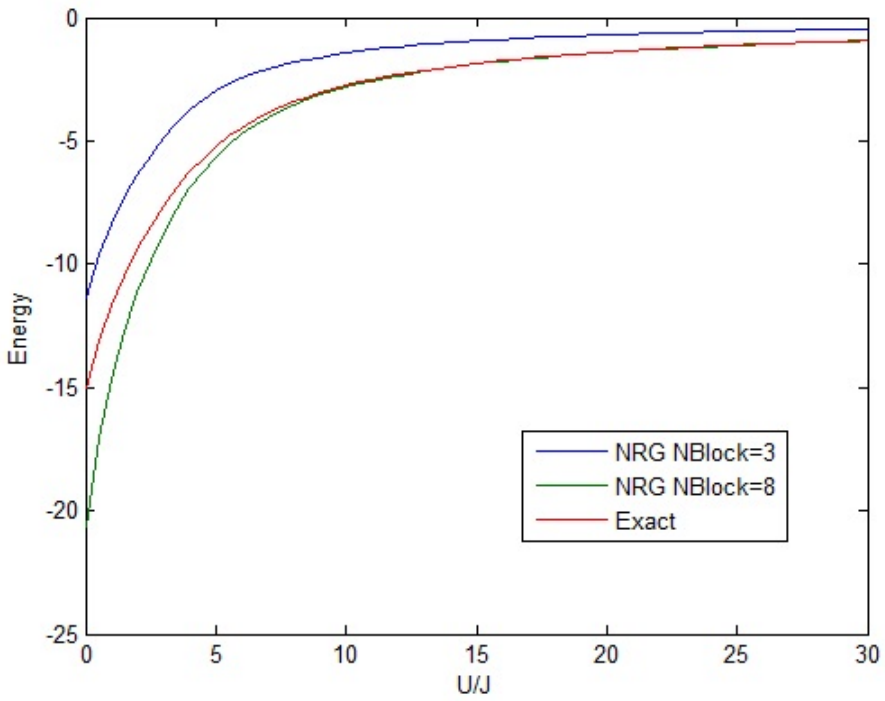

Figure 5: .Ground state as a function of the parameter U/J calculated using NRG method for initial range of particle numbers $0, 1, 2, 3$ and $0, 1, ...8$, for the case of filling factor 1 or $I = N = 8$ and the exact numerical solution

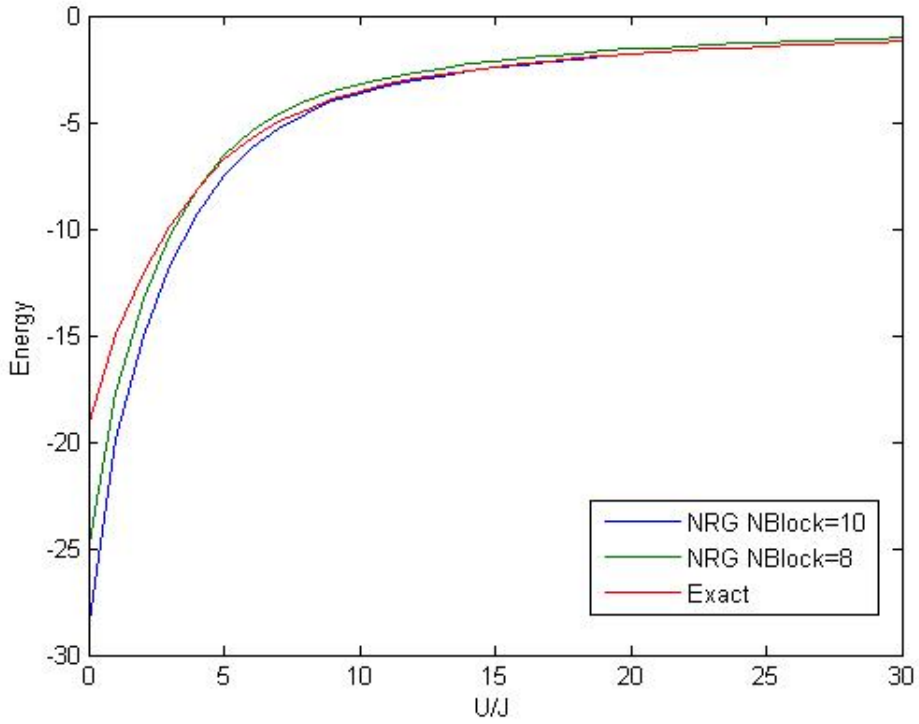

Figure 6: . Ground state as a function of the parameter U/J calculated using NRG method for initial range of particle numbers $0, 1, 2, ..8$ and $0, 1, ...10$, for the case of filling factor 1 or $I = N = 10$ and the exact numerical solution

Notice that the energies obtained using the NRG method converge to the exact result in the limit of strong interaction $U \gg J$, heuristically, this is because in the Mott insulator regime, the ground state consists only of a few eigenstates of the Hamiltonian with the interaction term dominating while in the superfluid regime the ground state consists of a superposition of all possible basis states many of which are discarded during the NRG process.

In Figs 7 and 8 we show the absolute deviation of the ground state calculated with the NRG method for different initial range of particle numbers to the exact numerical solution, again for $N = I = 8$ and $N = I = 10$. It can be seen that by increasing the initial basis dimension in the limit of high interaction there is an improvement of accuracy, as expected.

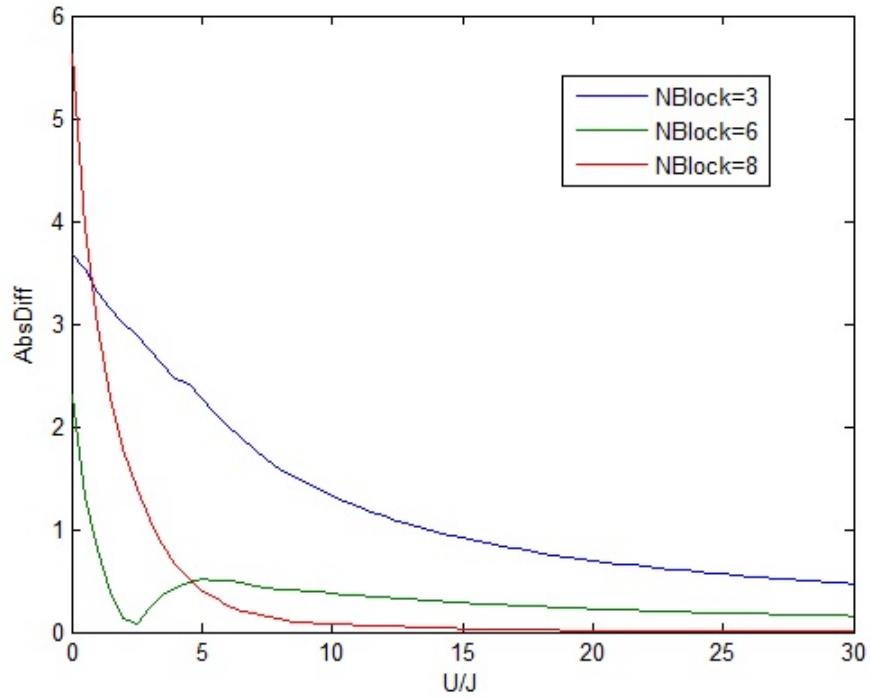

Figure 7: . Absolute Deviation of the NRG results to the exact numerical solution. Different initial range of particles for the NRG method are used.

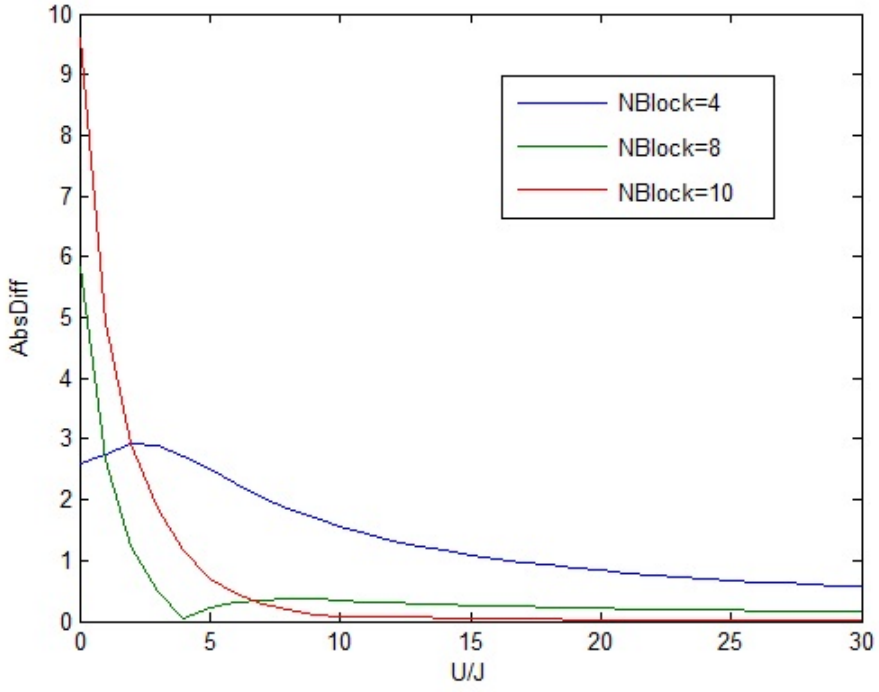

Figure 8: . Absolute Deviation of the NRG results to the exact numerical solution. Different initial range of particles for the NRG method are used.

The important point to notice is that (as shown in Table 1) for the case $N = 10$ the dimension of the Hilbert space is 92378 and the exact solution takes considerably much more time for running in comparison to the NRG algorithm.

2.3 NRG APPLIED TO THE SINGLE PARTICLE ON A TIGHT-BINDING MODEL

The NRG method was very successful when Wilson applied the procedure to the single impurity Kondo problem [31], also in the last section we saw that the NRG method gave good results for the Bose Hubbard model in the limit of high interaction $U \gg J$. Despite of this, the accuracy of the method becomes quite poor when applied to certain lattice models such as the Heisenberg model [32], particularly in comparison with other numerical approaches like Monte Carlo.

The application of NRG method to the problem of a single particle on a tight-binding chain [30] is quite useful in order to understand why the method breaks down in certain cases. We start considering the following Hamiltonian:

$$\hat{H} = -\sum_{i}^{L-1} (|i\rangle\langle i+1| + |i+1\rangle\langle i|) + 2\sum_{i}^{L} |i\rangle\langle i|, \tag{2.8}$$

where the state $|i\rangle$ corresponds to a localized tight-binding orbital on site i. When expressed in matrix form, the Hamiltonian takes the following form:

$$\hat{H} = \begin{pmatrix} 2 & -1 & 0 & 0 & \cdots \\ -1 & 2 & -1 & 0 & \cdots \\ 0 & -1 & 2 & -1 & \cdots \\ \vdots & \vdots & \vdots & \vdots & \end{pmatrix} \tag{2.9}$$

In this case it is reasonable to use the NRG procedure as described in the beginning of the chapter since for the present problem of a single particle the Hilbert space dimension is L for a lattice of length L and therefore it grows linearly with L. So, we fixed a truncation number m and start with two isolated blocks of dimension $L \geqslant m$ with Hamiltonian of the form Eq.2.9.

Then we create the Hamiltonian of the superblock composed of two identical blocks of length L. This super Hamiltonian will have the form:

$$\hat{H}_S = \begin{pmatrix} H_L & T_L \\ T_L^\dagger & H_L, \end{pmatrix} \tag{2.10}$$

where T_L represents the term that connects only sites on the block boundaries, i.e it has zeros everywhere, except for a -1 located at the lower left corner. Now, we can diagonalize H_L and truncate the basis to the m eigenvectors corresponding to the lowest eigenvalues. To do this, the usual transformation matrix O_L with these m eigenvectors as its columns is constructed. Hence, with $\overline{H}_L = O^\dagger H_L O$ and $\overline{T}_L = O^\dagger T_L O$ we construct the Hamiltonian for the next iteration:

$$H_{2L} = \begin{pmatrix} \overline{H}_L & \overline{T}_L \\ \overline{T}_L^\dagger & \overline{H}_L, \end{pmatrix} \tag{2.11}$$

and

$$T_{2L} = \begin{pmatrix} 0 & 0 \\ \overline{T}_L & 0 \end{pmatrix}. \tag{2.12}$$

The procedure is to be repeated until the desired system length is obtained. The numerical results are published in [30], and are shown in Fig.9. It is notable that the procedure performs quite badly after only a few iterations.

	Exact	Wilson	Fixed-Free
E_0	2.3508×10^{-6}	1.9207×10^{-2}	2.3508×10^{-6}
E_1	9.4032×10^{-6}	1.9209×10^{-2}	9.4032×10^{-6}
E_2	2.1157×10^{-5}	1.9214×10^{-2}	2.1157×10^{-5}
E_3	3.7613×10^{-5}	1.9217×10^{-2}	3.7613×10^{-5}

Figure 9: . Taken from [30]. Lowest energies after 10 iterations, $L = 2048$, $m = 8$. The second column is calculated with the NRG method. Third column with the White-Noack boundary procedure

Wilson exposed this example in 1986 at an informal seminar at Cornell University and explained the reason why the NRG method fails in this simple model. In the continuum limit, this model becomes the problem of a particle in a box of length L with infinitely high potential at the walls. The eigenfunctions for this problem are well known $\psi_n \sim \sin(n\pi x/L)$ with n a positive integer. The fundamental state is obtain with $n = 1$. The idea of the NRG is that the lowest eigenfunctions of the system at length L are combined to form the ground state of the system of length 2L. As shown in Fig 10, the ground state function of the 2L system has a kink in the middle which cannot be reproduced using the lowest eigenfunctions of dimension L, but nearly using all the states of the smaller block.

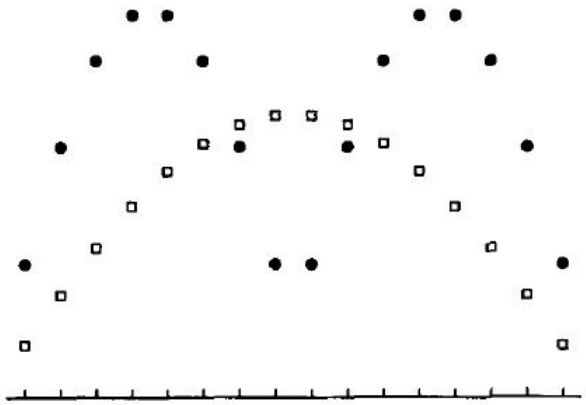

Figure 10: . Taken from [30]. Lowest eigenstates of two 8-site blocks (solid circles) and a 16 site block(open squares) for the one-dimensional tight-binding model with fixed boundary conditions.

The solution then lies on the treatment of boundary conditions: In the problem just described we used fixed boundary conditions which means that the eigenfunction vanishes at the end of the blocks. One way to solve the problem was proposed by White and Noack [30] by selecting the projecting states of the super Hamiltonian from the diagonalization of different blocks with different combinations of fixed and free boundary conditions, where the free boundary conditions are obtained by changing the diagonal matrix elements from 2 by 1 and results in the vanishing of the slope at the respective edge. We can form $H_L^{b,b'}$ with $b, b' =$ fixed or free, for instance for a 2 site block:

$$H^{free,fixed} = \begin{pmatrix} 1 & -1 \\ -1 & 2 \end{pmatrix}. \tag{2.13}$$

Diagonalizing this matrix we might choose the lowest $m/4$ eigenstates. Similarly, we construct $H_{free,free}$, $H_{fixed,free}$ and $H_{fixed,fixed}$ so that in the end we have a total amount of m non-orthogonal eigenstates that will serve to generate the projecting space. The transformation matrix can be built by orthonormalizing them, using the Gram-Schmidt procedure. We form the following reduced blocks $\overline{H}^{bb'} = O_L^\dagger H_L^{bb'} O_L$ and $\overline{T}_L = O_L^\dagger T_L O_L$; and finally create the Hamiltonian of size 2L:

$$H_{2L}^{bb'} = \begin{pmatrix} H^{b,fixed} & \overline{T}_L \\ \overline{T}_L^\dagger & H_L^{fixed,b'} \end{pmatrix}. \tag{2.14}$$

As can be seen from Fig 9 the ground energy obtained with this boundary account procedure gives results with an accuracy of nine digits. The method just described seems to work well for the case of the single particle problem but a generalization to interacting quantum lattice systems turns out to be difficult. In the next chapter, we study another approach developed by White in which the superblock is made out of the system of interest and its 'environment'. In contrast to the NRG method, the truncation is done by conserving the states of the system that are more entangled with the environment.

3

DENSITY MATRIX RENORMALIZATION GROUP

The Density Matrix Renormalization Group (DMRG) is a numerical technique based on the truncation of the Hilbert space of strongly interacting quantum lattice systems such as Heisenberg, t-J, and Hubbard models, used to calculate the ground and first excited states of the system. The algorithm achieves a very high precision even of the order of 10^{-9} for one-dimensional quantum systems within a reasonable computational effort. The roots of DMRG can be traced back to the Numerical Renormalization Group method developed by Wilson in 1975. As we mentioned in Chapter 2, this method fails to describe certain lattice systems like [32] Heisenberg and Hubbard models. In [28] White gave a heuristic argument to justify the modifications that have to be done to the NRG method in order to improve its results by using density matrix notation. In order to analyze which states to conserve during the truncation process, the system's block is embedded in some environment that will play the role of the thermodynamic-limit system in which in the end the block will be embedded. The argument is the following: For an isolated block at finite temperature or a block in thermal equilibrium with a bath at temperature T, the probability that the block is in an eigenstate α of the block Hamiltonian is proportional to $e^{-\beta E_\alpha}$ which is also an eigenvalue of the density matrix $e^{-\beta H_B}$. Therefore an eigenstate of the Hamiltonian is also an eigenstate of the density matrix and the eigenstates with the lowest eigenvalues of the Hamiltonian are the ones with the highest eigenvalues of the density matrix. In this way for an isolated block, the NRG method is a way to restrict the state of the system to the m most probable eigenstates of the density matrix. However, in general the block is not isolated and the density matrix is not $e^{-\beta H_B}$, therefore for a system which is strongly coupled with the environment, the generalization for finding the ground state would not be to keep the m lowest energy states of the system but the m eigenstates of the density matrix with the highest eigenvalues.

3.1 THEORETICAL APPROACH

There are several ways of approaching theoretically to DMRG method. Let us discuss two of them, following [23] and [28], in which they study the problem of approximating the state of a bipartite spin chain system (where the left side

represents the system of interest and the right side its environment) is studied. Let N_S,N_E be the dimensions of the Hilbert space for the system of interest and its environment, respectively; then, in general the state has the form $|\psi\rangle = \sum_{i=1}^{N_S}\sum_{j=1}^{N_E}\psi_{i,j}|i\rangle|j\rangle$, where $\{|i\rangle\}$, $\{|j\rangle\}$ are sets of orthonormal basis for the corresponding Hilbert spaces. White [28] found that if we want to approximate this state by a state of the form $|\widetilde{\psi}\rangle = \sum_{\alpha=1}^{m}\sum_{j=1}^{N_E} a_{\alpha,j}|\alpha\rangle|j\rangle$ where $|\alpha\rangle = \sum_{i=1}^{N_S}\mu_{\alpha,i}|i\rangle$ and $m < N_S$, then the "best" approximation is given when the $\{|\alpha\rangle\}$ states are the first m normalized eigenvectors of the reduced density matrix of the system (i.e those with the largest m eigenvalues). In this case the "best" approximation means to minimize $\||\psi\rangle - |\widetilde{\psi}\rangle\|$ with respect to $a_{\alpha,j}$ and $\mu_{\alpha,i}$:

$$\| |\psi\rangle - |\widetilde{\psi}\rangle\|^2 = 1 - 2\sum_{\alpha ij}\psi_{ij}a_{\alpha j}\mu_{\alpha i} + \sum_{\alpha j}a_{\alpha j}^2, \tag{3.1}$$

where we have assumed real coefficients for simplicity, $\langle\psi|\psi\rangle = 1$ and $\langle\alpha|\alpha'\rangle = \delta_{\alpha\alpha'}$. We derive with respect to $a_{\alpha j}$ and set the expression equal to zero as required for the minimization :

$$-2\sum_{i}\psi_{ij}\mu_{\alpha i} + 2a_{\alpha j} = 0, \tag{3.2}$$

therefore the condition for $a_{\alpha j}$ is $a_{\alpha j} = \sum_{i}\psi_{ij}\mu_{\alpha i}$ and replacing this in Eq.3.1 we obtain:

$$1 - \sum_{\alpha ii'}\mu_{\alpha i}\rho_{ii'}\mu_{\alpha i'} = 1 - \sum_{\alpha=1}^{m}\langle\alpha|\rho|\alpha\rangle \tag{3.3}$$

where $\langle i|\rho|i'\rangle = \rho_{ii'} = \sum_{j}\psi_{ij}\psi_{i'j}$, with ρ representing the reduced density matrix. Here we regard ρ as an Hermitian operator. Notice that, because it is positive definite, $\langle\alpha|\rho|\alpha\rangle \geqslant 0$ holds. Since we are looking for a minimum of the expression Eq.3.3 we need to look for the maximum value of every $\langle\alpha|\rho|\alpha\rangle$. The Rayleigh-Ritz principle establishes that for a Hermitian matrix H the extreme of $\frac{\langle\phi|H|\phi\rangle}{\langle\phi|\phi\rangle}$ with $|\phi\rangle = \sum_{i}^{n}x_i|\phi_i\rangle$ and $\{|\phi_i\rangle\}$ an orthonormal basis leads us to the condition $(H - \lambda I)\vec{x} = 0$, $\vec{x} \equiv (x_1, ..., x_n)^T$ which is an eigenvalue problem. By comparison, in our case this means that the mimimum of Eq. 3.3 is given by the m first $|\alpha\rangle$ eigenstates of ρ with highest eigenvalues.

Hence, the minimal distance squared is given by the *truncated weight*:

$$\||\psi\rangle - |\widetilde{\psi}\rangle\|^2 = 1 - \sum_{\alpha=1}^{m} \omega_\alpha \equiv \epsilon_\rho. \tag{3.4}$$

This quantity is important for calculating the error when evaluating the average of an arbitrary operator acting on the system using this sort of truncation. The reduced density matrix of the system $\hat{\rho} = Tr_E|\psi\rangle\langle\psi|$ with the N_S eigenvalues ω_α and orthonormal eigenstates $\hat{\rho}|\alpha\rangle = \omega_\alpha|\alpha\rangle$, $\sum_{\alpha}^{N_S} \omega_\alpha = 1$ is used to calculate the average of an observable $\hat{A}$ acting on the system:

$$\langle\hat{A}\rangle = Tr_S(\hat{\rho}\hat{A}), \tag{3.5}$$

expressing this equation in the eigenbasis of the density matrix and taking the trace over the system's Hilbert space we obtain:

$$\langle\hat{A}\rangle = \sum_{\alpha}^{N_S} \omega_\alpha\langle\alpha|\hat{A}|\alpha\rangle. \tag{3.6}$$

When projecting the system to the first m eigenvectors $|\omega_\alpha\rangle$, the approximated average is:

$$\langle\hat{A}\rangle_{approx} = \sum_{\alpha}^{m} \omega_\alpha\langle\alpha|\hat{A}|\alpha\rangle \tag{3.7}$$

and the error on $\langle\hat{A}\rangle$ will be bounded by:

$$|\langle\hat{A}\rangle - \langle\hat{A}\rangle_{approx}| = \sum_{\alpha>M_S}^{N_S} \omega_\alpha\langle\alpha|\hat{A}|\alpha\rangle \leqslant (\sum_{\alpha>m}^{N_S} \omega_\alpha)C_A \equiv \epsilon_\rho C_A \tag{3.8}$$

where $C_A \equiv max_\varphi|\langle\varphi|\hat{A}|\varphi\rangle| = \|\hat{A}\|$, with $\langle\varphi|\varphi\rangle = 1$. Therefore, for local quantities such as energy per site or magnetization, errors are of the order of the *truncated weight* after making this approximation.

3.1.1 *Using Schmidt Decomposition*

There is another way of approaching this idea of truncating the Hilbert space dimension taking into account a measure of entanglement between the system and

the environment. Let us create the $(N_S \times N_E)$ matrix A with A_{ij}=ψ_{ij}. We can use singular value decomposition in order to write $A = UDV^T$, where U is a unitary $(N_S \times N_S)$ matrix, D is an $(N_S \times N_E)$ diagonal matrix with non-negative elements and V is a $(N_E \times N_E)$ unitary matrix. Therefore a state can be written:

$$|\psi\rangle = \sum_{i,l'}^{N_S} \sum_{j,l}^{N_E} U_{il'} D_{l'l} V^T_{lj} |i\rangle|j\rangle = \sum_{l}^{N} \lambda_l \left(\sum_{i=1}^{N_S} U_{il} |i\rangle \right) \left(\sum_{j=1}^{N_E} V^T_{lj} |j\rangle \right),$$

where $N = min(N_S, N_E)$ and $D_{ll} \equiv \lambda_l$. We can define the following orthonormal vectors for the system and environment Hilbert space $|l\rangle_S = \sum_{i=1}^{N_S} U_{il}|i\rangle$, $|l\rangle_E = \sum_{i=1}^{N_E} V_{jl}|j\rangle$.

Expressing the state in this new basis we get the [19] *Schmidt decomposition*:

$$|\psi\rangle = \sum_{l}^{N_{Schmidt}} \lambda_l |l\rangle_S |l\rangle_E \quad N_{Schmidt} \leqslant min(N_S, N_E) \tag{3.9}$$

and we have replaced the $(N_S \times N_E)$ ψ_{ij} coefficients by the $N_{Schmidt}$ Schmidt coefficients; notice that since we started with a normalized state, then $\sum_l \lambda_l^2 = 1$. In the special case when $N_{Schmidt} = 1$ we can conclude that our state is separable as can be seen from Eq.3.9, otherwise we are dealing with an entangled state. An important characteristic of the Schmidt decomposition is that the reduced density matrices for the system and the environment are diagonal in this basis.

$$\hat{\rho}_S = \sum_{l=1}^{N_{Schmidt}} \lambda_l^2 |l\rangle_S \, {}_S\langle l| \quad \hat{\rho}_E = \sum_{l=1}^{N_{Schmidt}} \lambda_l^2 |l\rangle_E \, {}_E\langle l|. \tag{3.10}$$

Therefore, as expressed in [20] the reduced density matrix spectra gives clear information about the entanglement of a bipartite system. However, sometimes it is desirable to have a measure able to condense this information into one number. One way to obtain this is by using the generalization of the [19] von Neumann entropy to the reduced density matrices:

$$S_{vN} = -Tr\hat{\rho}_S ln\hat{\rho}_S = -\sum_{l=1}^{N_{Schmidt}} \omega_l ln\omega_l, \tag{3.11}$$

where $\omega_l \equiv \lambda_l^2$. Notice that whenever we have a separable state $S_{vN} = 0$, which is the minimum value of the entropy. On the contrary, the maximal value $S_{vN} = lnN$ is obtained when we have N equal non-zero eigenvalues: $\omega_n = 1/N$.

The idea of preserving only the m eigenstates of the reduced density matrix with the greater eigenvalues typically means to preserve the maximum possible entanglement between the system and the environment. [23] "While one may easily construct density matrix spectra for which upon normalization the truncated state produced by DMRG no longer maximizes entanglement, for typical density matrix spectra the optimization statement still holds in practice".

The natural question would be: For which cases and values of m are we able to get a good approximation for our initial state?. In [1], some possibilities are shown. For example, for certain states known as Matrix Product States (MPS), the density matrix spectra looks roughly like in Fig. 11:

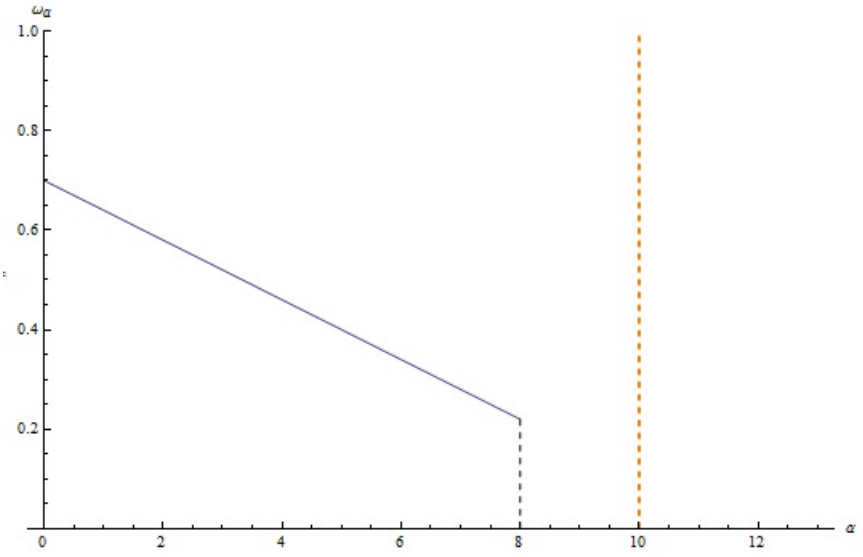

Figure 11: Sketch of the density matrix eigenvalues of a Matrix Product State.

In this case the approximation is exact since the value of m is greater that the number of eigenvalues different from zero.

In general, for many one-dimensional systems the density matrix spectra decays exponentially, as in Fig. 12:

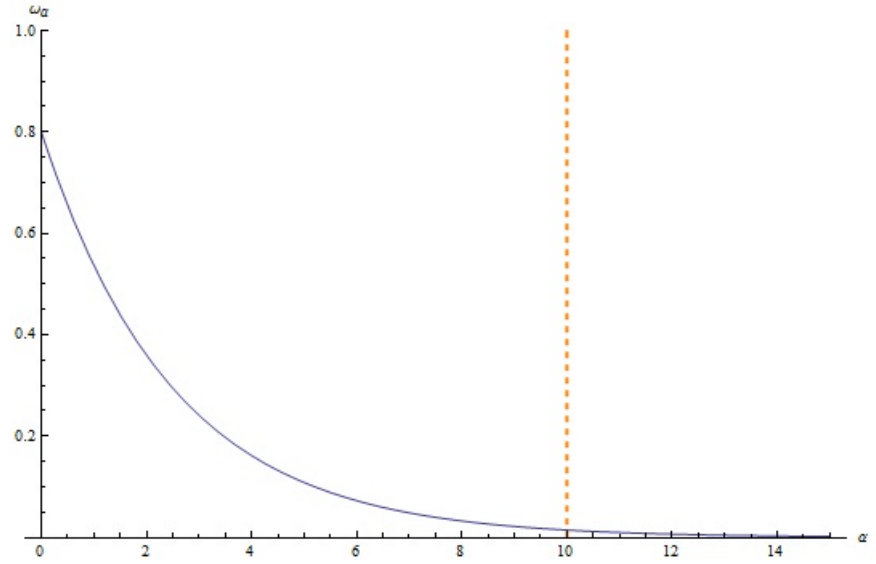

Figure 12: Sketch of the density matrix eigenvalues for a typical ground state of one-dimensional systems

Restricting the Hilbert space to the m states as shown, gives us a good approximation to describe the state of the system.

Finally a sketch for the spectral density for a typical ground state of a two-dimension system is shown in Fig. 13

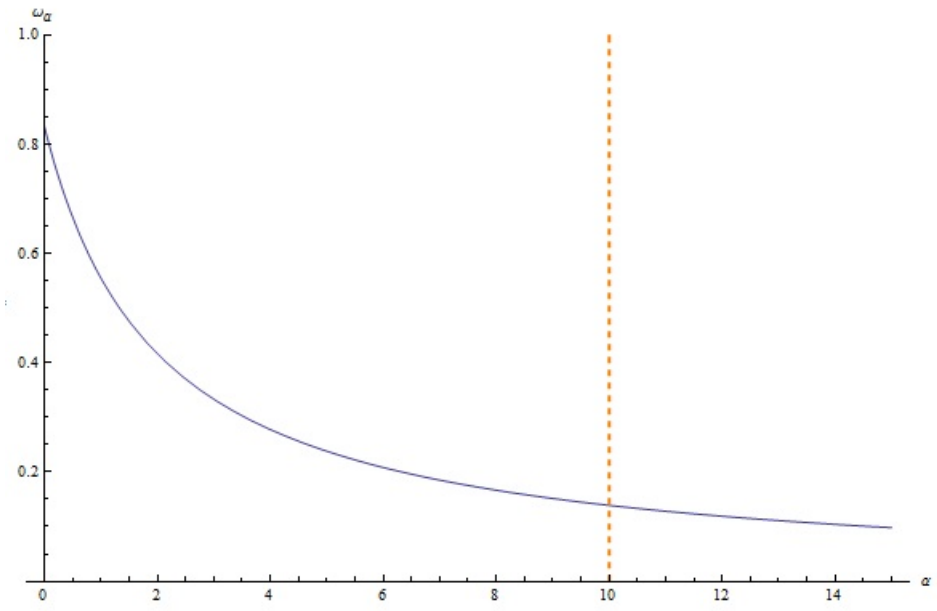

Figure 13: Sketch of a density matrix eigenvalues for a typical ground state of two-dimensional systems

In this case, the approximation is not good since many high entangled states would be excluded.

DMRG uses this way of approximating states, where the most important basis states in terms of system-environment entanglement are kept in order to study the fundamental states of one dimensional systems with neighboring interactions. The main idea is to keep the dimension of the Hilbert space fixed on which the approximated ground state lies even if the system is being enlarged.

3.2 INFINITE SYSTEM DMRG

Here we follow the prescriptions of [8], [23] and [28]. The infinite chain method is usually used when we want to study the ground state properties of infinite chains.

Let us start with a chain segment of L sites living on an m_L-dimensional Hilbert space $m_L \leqslant m$ with basis $\{|\alpha_L^B\rangle\}$, forming what we will call a system *block* and denote it as $\beta(L, m_L)$. It is possible to express in this basis our block Hamiltonian $\hat{H}_L^B$ and other local operators acting on it.

Then, we add one particle site to the system *block* so that the space of states of this *enlarged block* will have dimension dm_L and a basis formed by $\{|\alpha_B, \sigma\rangle\}$ where $|\sigma\rangle$ and d represent the basis and basis dimension for one particle in the system. With this enlarged basis we can construct the Hamiltonian for the enlarged system, $\hat{H}_{L+1}^E = \hat{H}_L^B + \hat{H}_L^S + \hat{H}^{BS}$ where $\hat{H}^{BS}$ is the interaction term between the added site and the block.

When our general Hamiltonian for the system presents global reflection symmetry, we can embed the *enlarged system block* into and identical environment E'. In this way, we are left with a chain of length $2L+2$ that we will reference to as the *superblock system* with its Hamiltonian operator given by $\hat{H}_{2L+2}^{Sup} = \hat{H}_{L+1}^E + \hat{H}_{L+1}^{E'} + \hat{H}^{EE'}$ (see Fig 14).

Once the *superblock* Hamiltonian is built in the product basis of dimension $d^2 m_L^2$, we proceed to diagonalize it in order to find the ground state $|\psi\rangle$ for the *super* system. There are some very efficient algorithms like [7] Davidson's and [14] Lanczos which allow us to obtain the ground state of the system up to a very good precision without having to compute the whole spectrum of the Hamiltonian.

Next, we form the reduced density matrix for the *enlarged block* $\hat{\rho}_E = \mathrm{Tr}_{E'}|\psi\rangle\langle\psi|$ so as to make the 'best' entangled approximation as described in the previous section. Therefore, we have to keep the $m_{L+1} = \min(m_L d, m)$ eigenstates of $\hat{\rho}_E$ with the greater eigenvalues. A $m_L d \times m_L$, matrix T of this truncated change of basis can be created, whose columns are the m_{L+1} eigenstates chosen before. The same can be done for the environment system.

Finally, we can make the reduced basis transformation to the *enlarged system* hamiltonian: $\hat{H}^{B}_{L+1} = T^{\dagger}\hat{H}^{E}_{L+1}T$ and also to the other local operators needed to implement the interaction term. Similarly for the environment system a truncated change of basis can be created in order to get $\hat{H}^{E'}_{L+1}$. Now, we are ready to repeat the algorithm so as to continue enlarging the system chain while keeping fixed the number of states used to describe it. For the next iteration our block will be denoted as $\beta(L+1, m_{L+1})$.

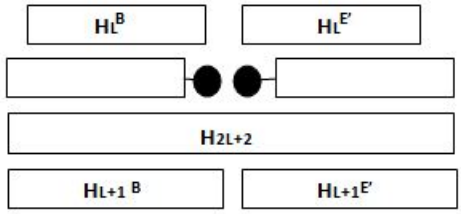

Figure 14: One Iteration of the DMRG infinite-system algorithm

3.3 FINITE SYSTEM DMRG

The finite system algorithm is used to study systems of finite length, the main idea of the algorithm being to choose the environment block in such a way that the size of the superblock is kept fixed during most of the iteration steps.

We start applying the infinite system algorithm until the desired length L of the superblock is attained. Since for the next algorithmic steps we will need the Hamiltonians that mimic the environments of all possible lengths up to L, in contrast to the infinite system procedure described in the last section, here it is necessary to store all the information about the Hamiltonian and boundary operators in each of the infinite system algorithm iteration. Now, we define a sweep or 'thermalization' and divide each of them into three steps.

- Once we have gotten the desired length , as can be seen in Fig 15, we are left with the block $\beta(L/2, m_{L/2})$. In order to keep the L dimension of the superblock for the next iteration, an environment block of length $L/2-2$ is needed. We use the second to last right block information stored during the infinite system algorithm. With the superblock Hamiltonian constructed we repeat the usual steps to make the renormalization: First calculate the superHamiltonian ground state, then calculate the reduced density matrix of the new left enlarged block and finally make the projection of this block on the subspace generated by the truncated eigenstates of the reduced density matrix. In this first part of the sweep the idea is to continue enlarging the left block

system and contracting the right block (for the right block, use the stored information) by developing the renormalization procedure until the length of the left block system is $L-3$. In each iteration replace the information just used for the right contracted block by that of the renormalized new enlarged block.

- The second part of the sweep consists on enlarging the right side while contracting the left side of the system. In every iteration the information of the left blocks stored during the first part of the sweep and the infinite system algorithm is used in order to construct the left environment blocks. Again, the dimension of the superblock is kept fixed and we replace the information of the new right enlarged blocks by that of the left blocks just implemented. In this Part we let the right block to increase its size from 1 to $L-3$, See Fig 15.

- Finally, we go back to a point with the same structure to the one that we started the sweep with. Therefore, in each iteration we need to construct the superblock with the just renormalized enlarged left block and the right block taken from the information stored in Part 2. We stop after performing the iteration where the length of the right and left blocks is $L/2-2$

At this point we are able to start another sweep again, typically the energy or observable under study converges after two of these sweeps.

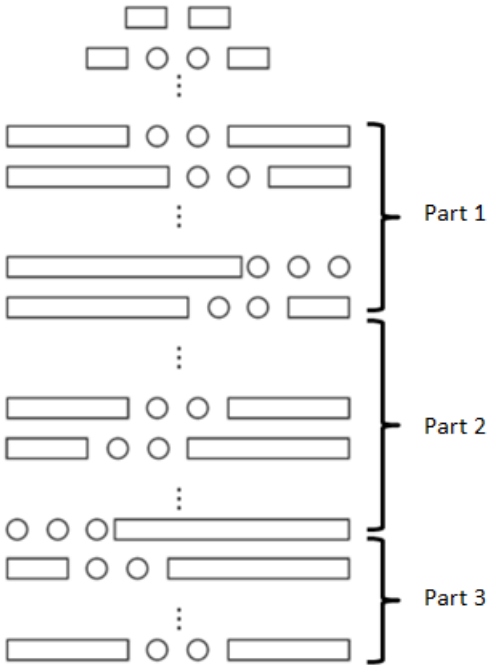

Figure 15: Sketch of one sweep in the Finite-system algorithm

3.4 PERIODIC BOUNDARY CONDITIONS

The DMRG algorithm, as we have explained until now, describes systems with open boundary conditions. Nevertheless, from a physical point of view, periodic boundary conditions are typically preferable to open ones, since surface effects are eliminated and for the exact solvable systems the solutions to compare DMRG results are easier to obtain with periodic boundary conditions.

In order to implement periodic boundary conditions the super block configuration is changed conveniently to that of Fig 16 where the two blocks are not neighbors. This configuration enhances the sparseness of the matrix Hamiltonian we have to diagonalize, compared to the standard configuration and therefore it improves the computational efficiency of the algorithm.

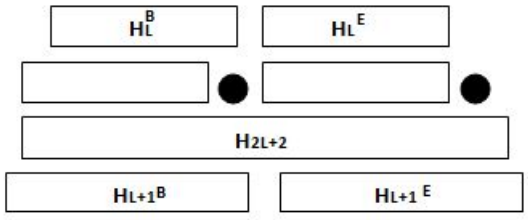

Figure 16: Superblock configuration for periodic boundary conditions.

The results for the periodic boundary conditions are much less precise than for open boundary conditions, see [28], [5] and [23]; away from criticality this is mainly because the spectra of the density matrices for periodic conditions decay slower than for the open boundary case off course affecting the precision of the DMRG algorithm. In [5] Chug and Peschel studied the density matrix eigenstates for the harmonic-oscillator model and they found that the density matrix eigenstates associated with the highest eigenvalues are mostly located close to the boundary between block and environment. Therefore, it is expected that increasing the boundary border as in the case of periodic boundary conditions will lead to a degeneracy of the highest eigenvalues affecting the DMRG performance.

3.5 RESULTS FOR THE HEISENBERG MODEL

We present the results obtained using our Matlab code for the DMRG algorithm applied to the Heisenberg antiferromagnetic model for S= 1/2, following [28]. See Apendix 3 for computational details. In Fig 17 we plot the first 22 density matrix eigenvalues ω_α in decreasing order for a 32 site system with open boundary conditions. It can be seen that it is possible to obtain a truncation weight of the order of 10^{-7} keeping only 22 states per iteration and therefore, as shown in Fig 17b not much improvement should be obtain with $m = 40$.

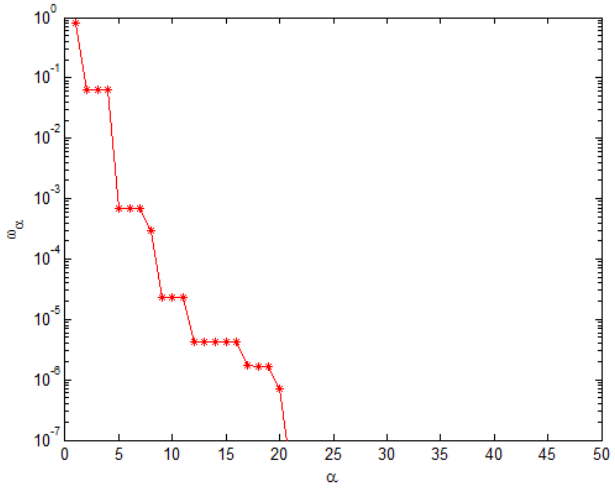

(a)

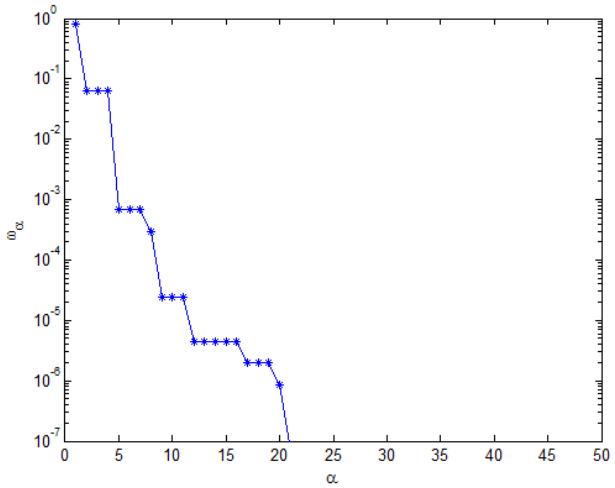

(b)

Figure 17: Density matrix eigenvalues ω_α vs eigenvalue index α for a 32 site system with open boundary conditions. (a) DMRG truncation number $m = 22$, (b) $m = 40$

In Fig 18 we show the relative error for the ground energy of the same 32 site system as a function of the number m of states kept. As suggested in [28] for the open boundary condition case the exact solution is calculated also with DMRG with $m = 58$.

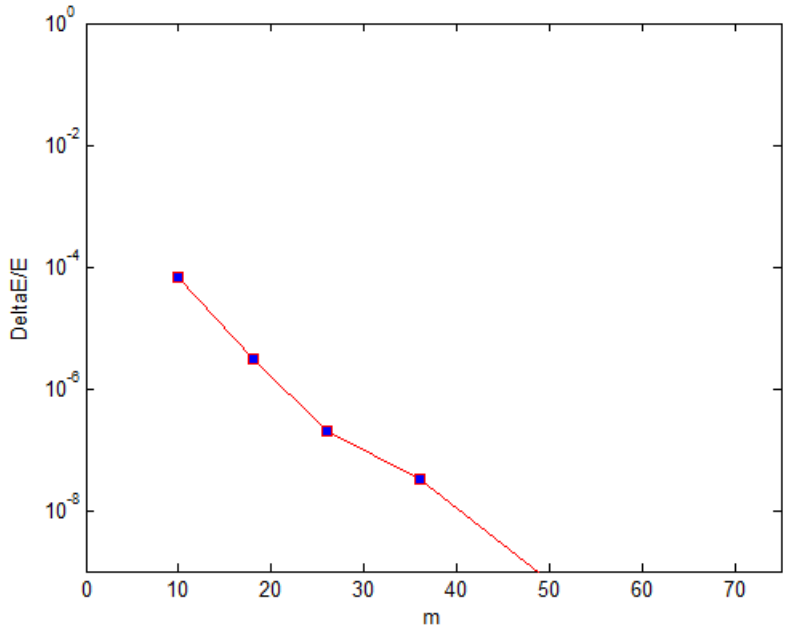

Figure 18: Relative error $\Delta E/E$ in the ground energy for a 32 site Heisenberg model with $S = 1/2$ as a function of the states kept m.

3.6 OTHER APPLICATIONS

Many other things are realizable with DMRG. For example, the lowest lying excitations can also be calculated with DMRG, in the same way we have explained for the ground state, see [23]. The best results are obtained when running DMRG for each level separately, which is done by diagonalizing the superblock and choosing the desired excitation.

Another way of doing it, all at once, is to calculate the reduced density matrix $\rho = \mathrm{Tr}_E \sum_i \alpha_i |\psi_i\rangle\langle\psi_i|$, where the sum goes over the few excited states and the ground state. The α_i are such that $\sum_i \alpha_i = 1$ and are equally weighted.

Furthermore, DMRG allows us to compute expectation values of observables with respect to the calculated ground state, See [23] and [8]. The simplest case is when performing the DMRG finite algorithm and we want to measure a local observable $M(i)$. We have to select the step inside the last sweep such that one of the two free sites is i. Hence, if the calculated ground state at this point is $|\psi\rangle = \sum \psi_{i_1,i_2,i_3,i_4} |i_1, i_2, i_3, i_4\rangle$, i_1, i_2, i_3, i_4 denoting the basis of the left block, the two free sites and the right block respectively, the expected value is given by:

$$\langle\psi|M(i)|\psi\rangle = \sum \psi^*_{i_1,i_2,i_3,i_4} M(i)_{i_2,i_2'} \psi_{i_1,i_2',i_3,i_4}. \tag{3.12}$$

It is also possible to evaluate $M(i)$ using the infinite DMRG algorithm. When i is not representing one of the two central free sites of the last iteration, it is necessary to update $M(i)$ in each of the new basis generated at every iteration: $M(i) \rightarrow T^{\dagger}M(i)T$. Other kind of observables like correlation functions can also be computed. These sort of calculations have more subtleties, we suggest the interested reader to look at [23] for a complete explanation.

In the next chapter we will use our DMRG codes to characterize the reduced density spectrum of one dimensional chains with XY interaction, we will be able to explore the advantages and limitations of the algorithm in this context.

4

SCHMIDT GAP AS AN ORDER PARAMETER

Using DMRG algorithm, we follow [9] to show that for the XY model, the behavior of the Schmidt gap close to the quantum phase transition is the same as that of an order parameter. First we make a brief review about thermal and quantum phase transitions. We follow [33], [10] and [3], then we give the results obtained by implementing Finite Size Scaling analysis for the Schmidt gap in the case of the transverse Ising model with and with out perturbation and in the case of the anysotropic XY model when $\gamma = 0.5$.

4.1 QUANTUM PHASE TRANSITIONS

Quantum Phase Transitions (QPT) are phase transitions that occurred at zero temperature, driven by quantum fluctuations when moving non thermal parameters, in opposite to the well known thermal phase transitions which are triggered by fluctuations generated by moving the temperature close to a critical point T_c.

Let us review some features of the thermal phase transitions that are useful to study QPT. They can be of first or second order depending on the analytic behavior of one of the thermodynamic potentials, such as the free energy. If the potential has a discontinuity in one or more of it's first derivatives, for instance in the magnetization function, then it is said to be of first order. On the other hand, if the first derivatives are continuous but second derivatives are discontinuous or diverge, the transition will be of second order.

Thermodynamic variables give macroscopic information about the state of the system, usually it is also important to consider microscopic variables to get a deep understanding about the system. For a ferromagnetic system, the correlation function is defined to measure the correlation between the spins on sites i and j,

$$G_{ij} = \langle S_i S_j \rangle - \langle S_i \rangle \langle S_j \rangle, \tag{4.1}$$

away from the critical point this function decays exponentially with the distance between the spins and for a translation invariant system we have:

$$G(\vec{r}) \sim C(r) exp(-r/\xi), \tag{4.2}$$

where ξ is known as the correlation length. Close to the critical point long range order develops in the system and the correlation length diverges as $\xi \sim |T - T_c|^{-\nu}$ and Eq. 4.2 becomes invalid. Experiments and soluble models show that at criticality the correlation function decays as a power law $G(\vec{r}) \sim r^{d-2+\eta}$.

An order parameter is a quantity that allows us to distinguish among different phases of the system. For a ferromagnetic system the magnetization is an order parameter; we will see that in certain cases the Schmidt gap can also serve as an order parameter. Let $\mathcal{O}(\vec{x})$ be an order parameter, then $\langle \mathcal{O}(\vec{x}) \rangle = 0$ for $T \geqslant T_c$ and $\mathcal{O}(\vec{x}) \neq 0$ for $T < 0$. When $T \to T_c$ the order parameter approaches zero as $\langle \mathcal{O}(\vec{x}) \rangle \sim (T_c - T)^{\beta}$. Other quantities like the specific heat and the susceptibility diverges as $C \sim (T - T_c)^{-\alpha}$ and $\chi \sim (T - T_c)^{-\gamma}$ respectively. At $T = T_c$ the order parameter scales with the magnetic field as $\langle \mathcal{O}(\vec{x}) \rangle \sim h^{1/\delta}$ for $h \to 0$.

This six critical exponents $(\alpha, \beta, \gamma, \delta, \nu, \eta)$ are connected by the four scaling relations:

$$\gamma = \nu(2-\eta), \qquad \alpha = 2 - \nu D, \qquad 2\beta = \nu(D-2+\eta), \qquad \delta = \frac{D+2-\eta}{D-2+\eta}. \tag{4.3}$$

The special feature of criticality is that the correlation length is infinite and that the critical system is invariant under all length scales. Phase transitions that present the same critical behavior (same critical exponents) are said to belong to the same universality class, which are determined by the dimension of the system and by the symmetries of the Hamiltonian and do not depend on it's microscopic details.

Now, consider a lattice system at $T = 0$ with a Hamiltonian given by:

$$H = H_o + gH_1 \tag{4.4}$$

with $[H_o, H_1] \neq 0$. For a finite lattice system there could be an avoided level crossing between the ground and the first excited state, this, can become an actual level crossing in the thermodynamic limit. At this point, the energy function $E(g)$ becomes non analytic showing an undergoing QPT.

When $g \ll 1$, H_o is the dominant term and the ground state will be essentially that of the H_o with some perturbative quantum fluctuations; on the contrary, when $g \gg 1$ the ground state will be dominated by H_1.

For a QPT the scaling relations of Eq. 4.3 have to be modified. In [3] this is done by introducing the concept of imaginary time so that the mapping from quantum to classical systems can be done. In [17], [22] the partition function for a D-dimensional quantum system is the following:

$$Z = \mathrm{Tr}\, e^{-\beta H}, \tag{4.5}$$

the trace can be evaluated in a complete set of states $|\{\phi\}\rangle$ such that:

$$Z = \sum_{\phi} \langle\{\phi\}|e^{-\beta H}|\{\phi\}\rangle. \tag{4.6}$$

The interesting feature here is that when we associate to β an imaginary time $t \to -i\beta$, the operator $e^{-\beta H}$ can be seen as an evolution operator e^{-iHt} and the partition function as the sum of the amplitude matrix elements that bring the basis states into it's original state after the time evolution.

Furthermore, when taking the thermodynamic limit and $T \to 0$ $(\beta \to \infty)$ necessary for a QPT to happen, we are extending the system to an infinite extent in it's D-dimensional space plus the imaginary time dimension. This is effectively a $(D+1)$ dimensional classical model.

Same as in thermal phase transitions the correlation length will diverge as $\xi \sim |g - g_c|^{-\nu}$ when $g \to g_c$. In addition, an imaginary time correlation length can be defined ξ_τ, which also diverges at criticality and for a second order transition behaves like:

$$\xi_\tau \sim \xi^z \sim |g - g_c|^{-\nu z} \tag{4.7}$$

where z is known as the dynamic critical exponent. For the one dimensional transverse Ising model that we are going to treat in the next section $z = 1$. It can also be shown [3] that $\xi_\tau \sim \Delta^{-1}$, where Δ is the energy gap between the ground and first excited state.

Taking this into account, the generalization of the scaling relations Eq. 4.3 is: (See [3]):

$$\begin{aligned} \gamma &= \nu(2-\eta), & \alpha &= 2-\nu(D+z), \\ 2\beta &= \nu(D+z-2+\eta), & \delta &= \frac{D+z+2-\eta}{D+z-2+\eta}; \end{aligned} \tag{4.8}$$

since $D \to D+z$ and not to $D+1$ as could be expected when mapping the D dimensional quantum system to a $D+1$-dimensional classical system.

To finish this brief overview of QPT, let us discuss in general terms the effects of a QPT at finite temperatures. It is possible to introduce a frequency ω_c such that $\Delta \sim \hbar\omega_c$. Quantum mechanics is important whenever the temperature is low enough so that $K_B T < \hbar\omega_c$.

[10] Two types of phase transitions are possible at this point, depending on the existence of a thermal phase transition besides the QPT. These are shown in Fig. 19.

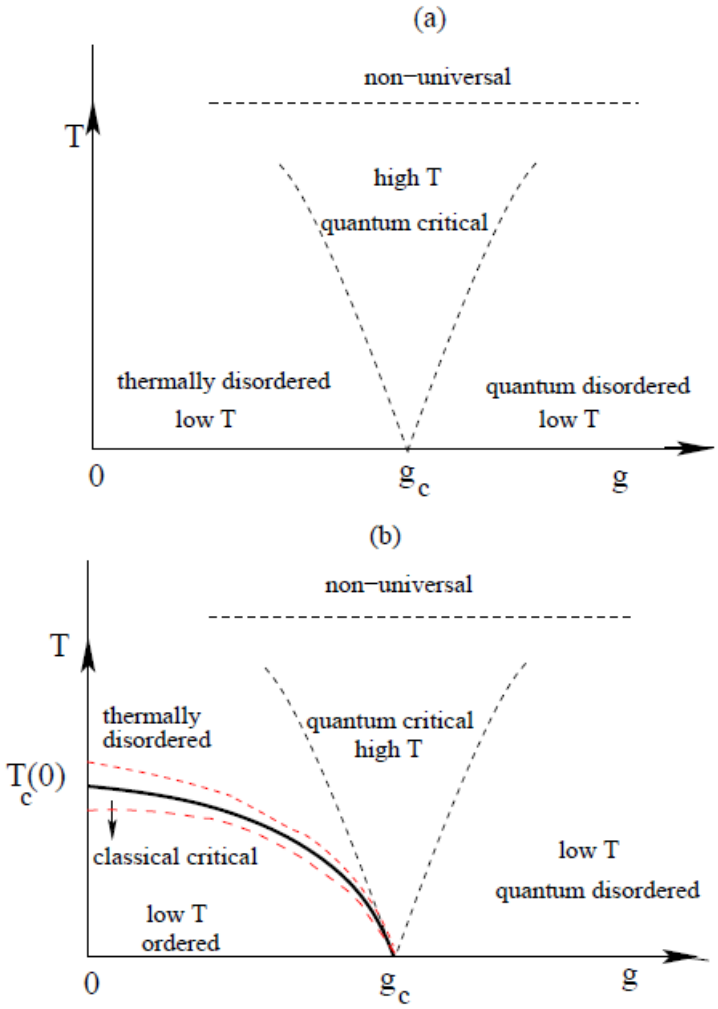

Figure 19: Taken from [10]. Two Types of phase diagrams close to the quantum critical point. (a) Only a QPT occurs at $g = g_c$. (b) Case where an ordered phase exists even at $T \neq 0$.

In Fig. 19 (a) the system presents only a phase transition at $T = 0$, this is the case for the one dimensional transverse Ising model for which no phase transition at any finite temperature occurs. Despite of this, the three regions shown in the figure characterize the nature of the fluctuations (thermal or quantum) that destroy the long range order. In the quantum critical region, both fluctuations are important. For the one dimensional transverse Ising model $g = B_z/J$ with B_z the transverse magnetic field and J the spin-spin interaction, (in the next section we change to $g = J/B_z$) this means for $g > g_c$ at low temperature, the disordered is generated by the term in the Hamiltonian accompanying the transverse magnetic field and for $g < g_c$ thermal fluctuations destroy the possible order that could be generated by having $g < g_c$.

Even though we are not going to treat with systems having a phase diagram similar to that of Fig. 19 (b), we explain it briefly. The solid line in Fig.19 (b) marks the difference between the ordered and the disordered phase that exists also for finite temperature. This is the case for the two dimensional transverse Ising model. At $g = 0$ $(B_z = 0)$ and $T = T_c(0)$, the thermal phase transition is that one of the two dimensional classical Ising model. On the other hand, the crossover from the low T quantum disordered region to the high T quantum critical region is characterize by the condition $\hbar\omega \sim K_B T$.

After this overview of QPT, next section explains the possibility of considering the Schimdt gap as an order parameter of at least one dimensional systems.

4.2 SCHMIDT GAP AS AN ORDER PARAMETER

In this section we follow [9] to show that for the one dimensional transverse Ising model with and without longitudinal perturbation, the Schmidt gap $\Delta\lambda = \lambda_1 - \lambda_2$ (with λ_i the two highest eigenvalues of the reduced density matrix) can be seen as an order parameter of the undergoing QPT i.e $\Delta\lambda$ scales same as the magnetization of the system. The Hamiltonian for the model just mentioned is:

$$H = -J \sum_i \sigma_x^i \sigma_x^{i+1} - B_z \sum_i \sigma_z^i + B_x \sum_i \sigma_x^i \tag{4.9}$$

with $\sigma_{k=x,y,z}$ denoting the Pauli matrices.

Let us in first place focus on the model without longitudinal perturbation, that is $B_x = 0$, the remaining Hamiltonian is invariant under the $\mathbb{Z}_2$ symmetry $\sigma_x^i \to -\sigma_x^i$, $\sigma_y^i \to -\sigma_y^i$ and $\sigma_z^i \to \sigma_z^i$, which can be implemented via the inner automorphism $\sigma_k^i \to \sigma_z^i \sigma_k^i \sigma_z^i$. As explained in the former section, quantum fluctuations are created due to the non commuting of the two terms in the Hamiltonian and a QPT is induced from an ordered phase (FM) to a disordered paramagnetic (PM) phase. [3] It can be seen by mapping the one dimensional quantum system to a classical $(1+1)$ Ising system that a QPT occurs when $J/B_z = 1$. Consequently, [10], [22] in the thermodynamic limit for $J/B_z < 1$ the magnetic field term dominates and $M_x = \frac{1}{L}\sum_i \langle \sigma_x^i \rangle = 0$, on the other hand, when $J/B_z > 1$ the system is in a (FM) phase $M_x \neq 0$. For $B_z = 0$ there are two degenerate ground states given by $|\rightarrow\rangle = \prod_i |\rightarrow\rangle_i$ and $|\leftarrow\rangle = \prod_i |\leftarrow\rangle_i$; $|\rightarrow\rangle$, $|\leftarrow\rangle$ the eigenvectors of σ_x. In this case, the $\mathbb{Z}_2$ symmetry transformation generated by $\prod_i \sigma_z^i$, maps the two ground states into each other. In a thermodynamic system one of the two states is chosen as the ground state which is usually preferred due to some external perturbation; this

is known as spontaneous symmetry breaking. In the vicinity of the critical point $J/B_z \to 1^+$, the magnetization goes to zero as a power law $M_x \sim (J/B_z - 1)^\beta$ and the correlation length diverges $\xi \sim |J/B_z - 1|^{-\nu}$, where $\beta = 1/8$ and $\nu = 1$, which coincide with the critical exponents of the two dimension classical Ising model.

In reference [9] the entanglement spectrum for open boundary conditions is computed, employing Jordan Wigner and Bogoliubov transformations to map the transverse Ising model into a system of noninteracting fermions. Then, they follow [20] to calculate the spectrum of the reduced density matrix for half of an L long chain. In general, the analytic solution for the XY model has been exposed in [16] by performing Wigner-Jordan, Fourier and Bogoliubov transformations. However, we have worked with open boundary conditions because our DMRG code has been developed for this situation. We have followed [18] and [20] to compute numerically the exact entanglement spectrum and reproduce the results obtained in [9].

The results for the entanglement spectrum of the first eight eigenvalues as a function of the parameter $g = J/B_z$ are plotted in Fig. 20 , showing that for the ferromagnetic phase there is a tendency of $\Delta\lambda$ to collapse close to $g_c = 1$. Furthermore, in Fig. 21 we observe that the collapsing happens closer to g_c when the system size is increased; we have plotted this behavior for $L = 768, 1536, 3072, 6000, 8000$.

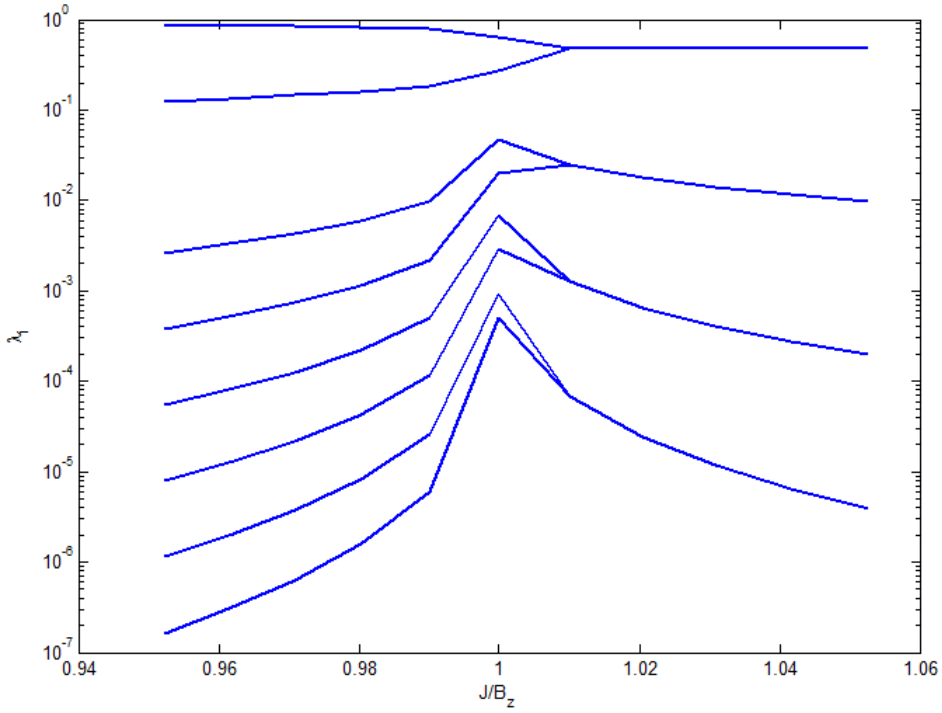

Figure 20: One dimensional Transverse Ising model. First 8 eigenvalues of the reduced density matrix for half segment of the chain as a function of $g = J/B_z$ for $L = 6000$.

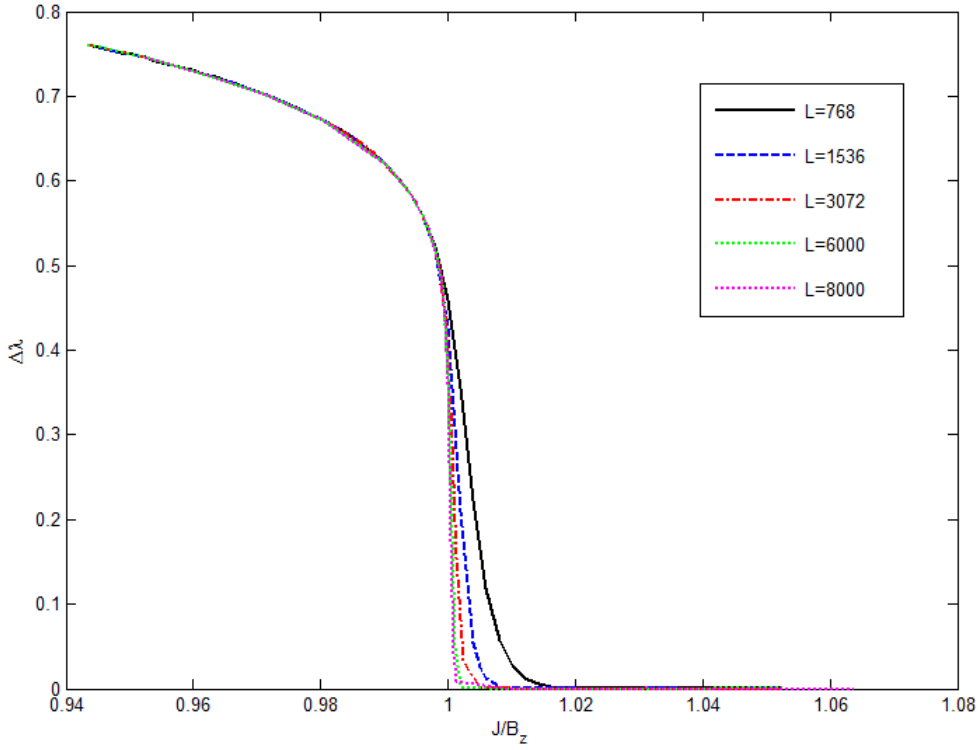

Figure 21: One dimensional Transverse Ising model. Schmidt gap as a function of J/B_z for $L = 768, 1536, 3072, 6000, 8000$ different lengths.

Due to the fact that the QPT occurs only in the thermodynamic limit and the numerical computations are develop for finite chains in [9], the finite size scaling theory is implemented in order to retrieve the asymptotic behavior of the system. Finite size scaling theory predicts the following relation near the critical point between the order parameter Q and the finite size chain:

$$Q(L, g) \simeq L^{-\beta_Q/\nu} \bar{Q}(|g - g_c|^{1/\nu}), \tag{4.10}$$

where ν and β are the exponents characterizing the behavior of the correlation length and the order parameter respectively.

On the basis of the Renormalization Group Theory [33], [17] Eq. 4.10 can be justified. The salient point is to include an additional scaling field $K_o = 1/L$ to the standard Renormalization Group procedure [25], [12].

Far from criticality when $\xi < L$ the system behaves like an infinite system and the measurement of physical quantities like the magnetization M or the susceptibility χ is independent of the lattice size. On the contrary, in the vicinity to criticality where the correlation length is comparable to the size of the system i.e $\xi \sim L$, the values of the quantities mentioned above present a size dependency and differ from

those of the infinite system. The finite size scaling expression for the magnetization reads: [12]

$$M \simeq L^{-\beta_Q/\nu}\bar{M}((g-g_c)^{1/\nu}). \tag{4.11}$$

In Eq. 4.10 we adopt the form of Eq.4.11, it might be satisfied by the Schmidt gap, with $Q \sim |g-g_c|^{\beta_Q}$ if this happens to be an order parameter. Let $\mu_1 = \beta_Q/\nu$ and $\mu_2 = 1/\nu$, so that $\Delta\lambda\, L^{\mu_1} \simeq \bar{\Delta\lambda}(|g-g_c|\, L^{\mu_2})$; in order to obtain the critical exponents, the coefficients μ_1 and μ_2 are changed until the graph of $\Delta\lambda\, L^{\mu_1}$ vs $|g-g_c|\, L^{\mu_2}$ collapse in the same function for different values of L. The results are shown in Fig. 22 and the critical exponents are calculated as $\beta_{\Delta\lambda} = 0.124 \pm 0.002$ and $\nu_{\Delta\lambda} = 1.00 \pm 0.01$, which turns out to coincide with those of the two dimensional Ising universality class mentioned above.

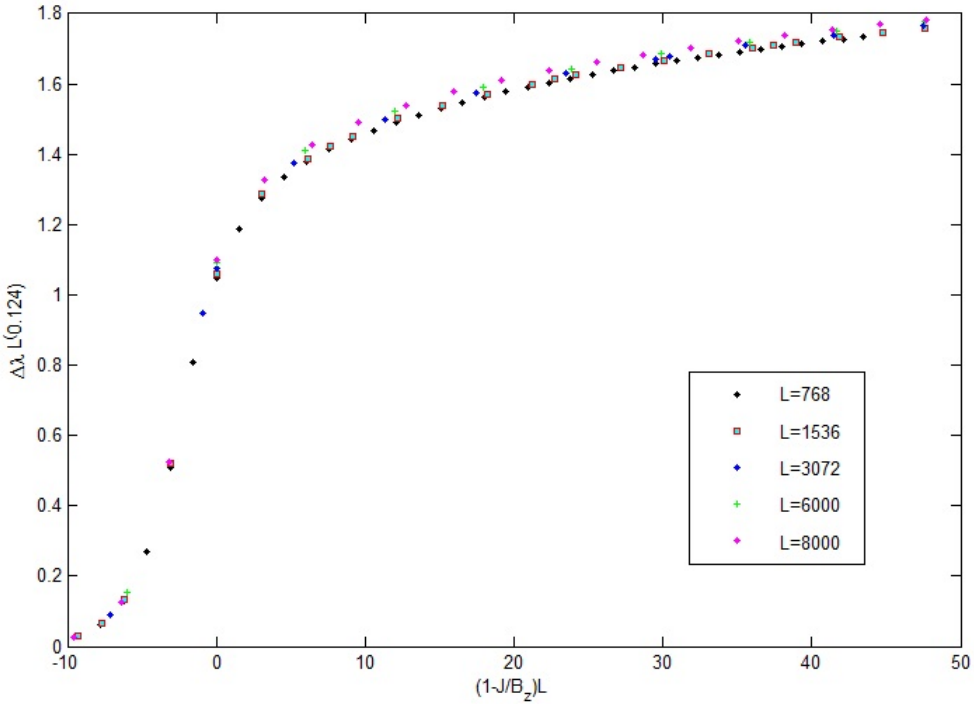

Figure 22: One dimensional Transverse Ising model. Finite Size Scaling analysis for $L = 768, 1536, 3072, 6000, 8000$

From Fig. 20 we observe that the entanglement spectrum becomes degenerated for the smallest values of B_z. Furthermore, from Fig. 21 we see that the degeneracy starts getting closer to the value $J/B_z \to 1^+$ as L increases. When we used our DMRG code to calculate the highest values of the spectrum of the partial density matrix of chains of different length in the regions where the spectrum is not yet degenerated, we obtained very good results as shown in Fig 23, 24.

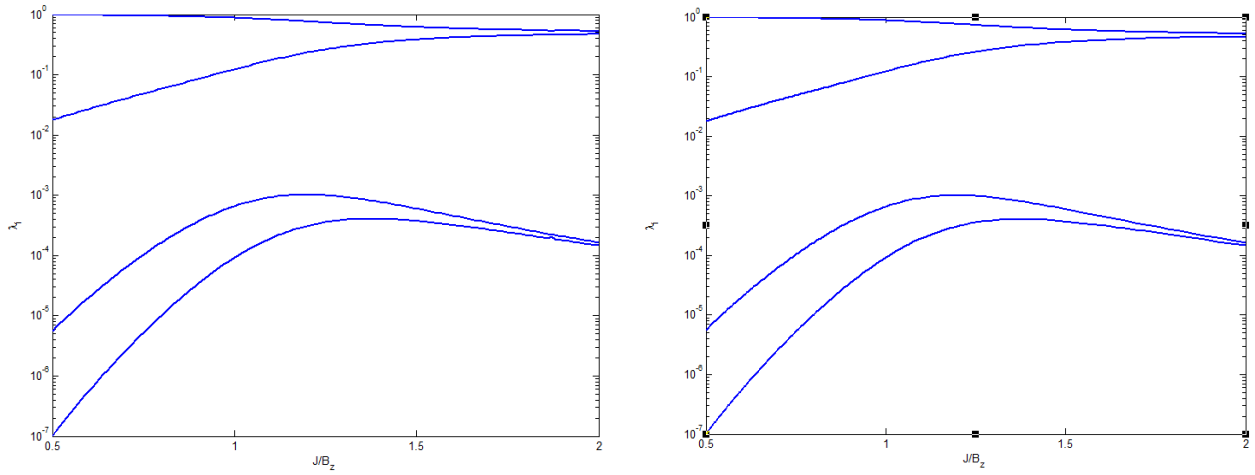

(a) (b)

Figure 23: Highest eigenvalues of the partial density matrix for $L = 10$ calculated with (a) DMRG , (b) Exact Numeric Method

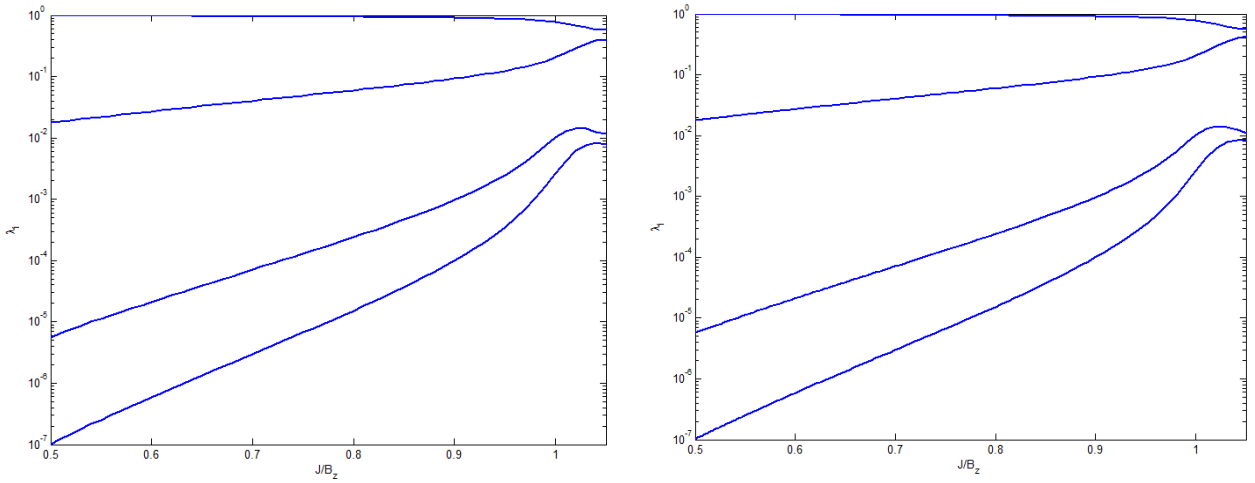

(a) (b)

Figure 24: Highest eigenvalues of the partial density matrix for $L = 100$ calculated with (a) DMRG , (b) Exact Numeric Method

Using DMRG for a chain of length $L = 604$, it is evident from Fig. 25 that it is not able to obtain the degeneracy in the reduced density matrix spectrum. We suspect that this problem is mainly due to computational issues when choosing the ground state in each iteration of the DMRG algorithm, since in this region (small values of B_z) the ground state and the first excited state turn out to be very close to each other.

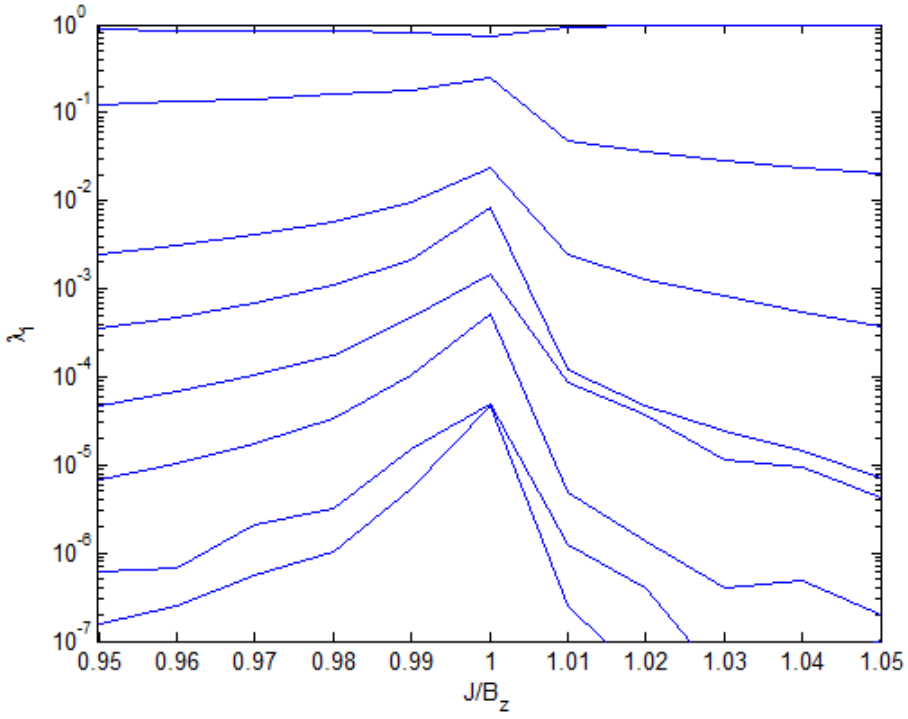

Figure 25: One dimensional Transverse Ising model. First 8 eigenvalues of the reduced density matrix for half segment of the chain as a function of $g = J/B_z$ for $L = 604$, computed with DMRG code.

However, our results look very similar to those of Fig. 20 when $J < B_z$. We performed the Finite Size Scaling analysis by approaching to the critical point as $J/B_z \to 1^-$, see Fig.26. We observe the collapsing curve obtained in Fig.26 matches that of Fig.21 for $J < B_z$.

The transverse Ising model can be seen as a particular case of the XY model. The expression for the Hamiltonian is:

$$H = -J \sum (\frac{1+\gamma}{2})\sigma_x^i \sigma_x^{i+1} + (\frac{1-\gamma}{2})\sigma_y^i \sigma_y^{i+1} - \sum \lambda \sigma_z^i. \tag{4.12}$$

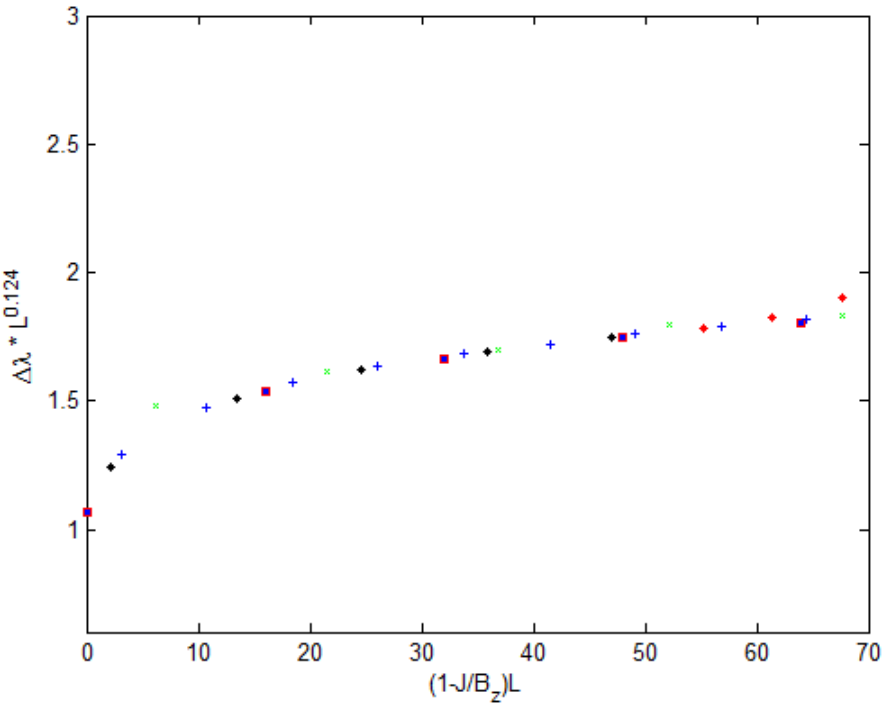

Figure 26: One dimensional transverse Ising model. Finite Size Scaling analysis for $L = 400$ Red-Square, 560 Black $*$, 768 Blue $+$, 1536 Green x, 3072 Red $*$, computed with DMRG code.

Two critical regions [16] are found in the parameter space. The line given by the XX model $\gamma = 0$, $\lambda \in [0, 1]$ and the line $\lambda = 1$, $\gamma \in (0, 1]$, see Fig.27. These two critical regions define two different universality classes.

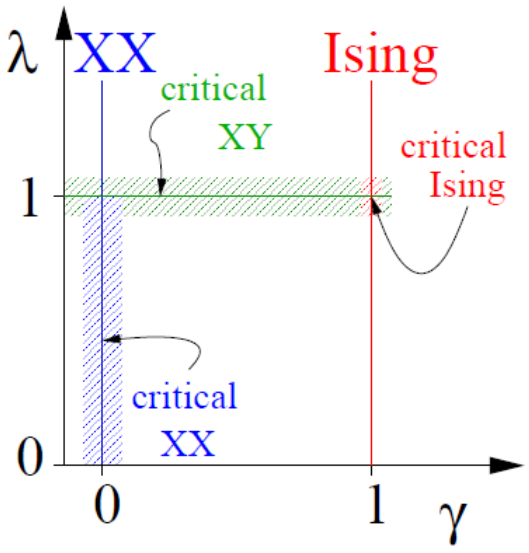

Figure 27: Taken from [16]. Critical regions of the XY model for the parameter space (γ, λ)

Since the system for $\gamma = 0.5$ belongs to the same universality class than that for $\gamma = 1$, we plotted for $\gamma = 0.5$ the reduced density spectrum for half chain close to the critical point.

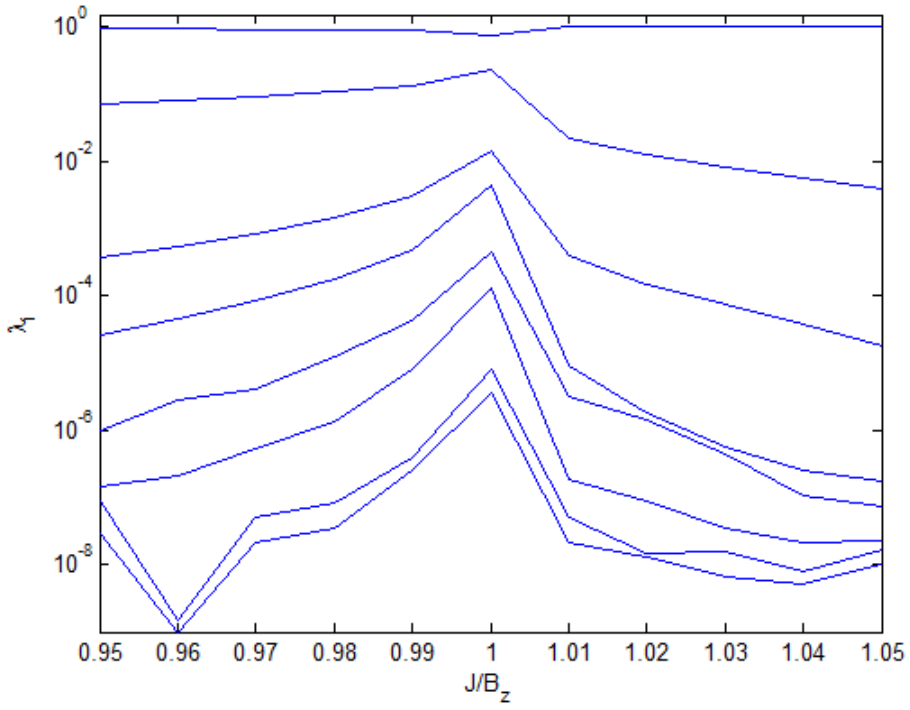

Figure 28: One dimensional XY model $\gamma = 0.5$. First 8 eigenvalues of the reduced density matrix for half segment of the chain as a function of $g = J/B_z$ for $L = 604$, computed with DMRG code.

The Finite Size Scaling analysis is also presented in Fig. 29. As expected, the collapsing curves for $\gamma = 1$ and $\gamma = 0.5$ are the same since they are characterized by the same critical exponents.

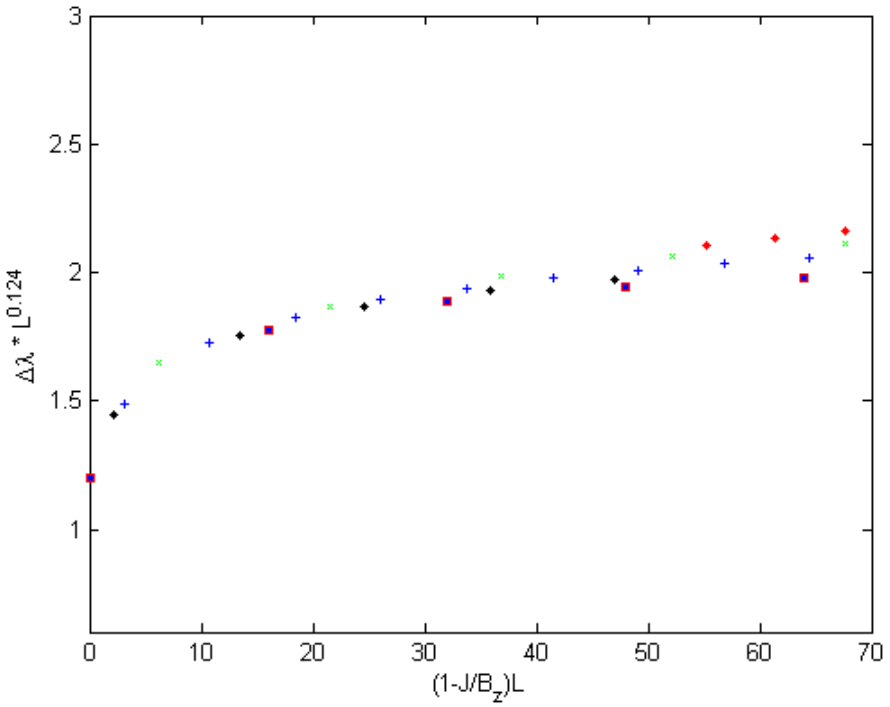

Figure 29: One dimensional XY model $\gamma = 0.5$. Finite Size Scaling analysis for $L = 400$ Red-Square, 560 Black $*$, 768 Blue $+$, 1536 Green x , 2000 Red $*$, computed with DMRG code.

Two important things have to be commented around the "effectiveness" of DMRG with respect to the behavior of the entropy in different regions of the parameter space of Fig. 27. As we saw in Chapter 3, the entanglement entropy gives information about the reduced density matrix spectrum. To code the information of S_L in DMRG we will need a Hilbert space of size $M \geqslant 2^{S_L}$ [23]. For one dimensional systems, in particular for the one dimensional Transverse Ising model, in **??** entanglement entropy is calculated for a chain of size L embedded in an infinite chain, see Fig. 30. At the critical region $\lambda = 1$ the entropy scales logarithmically with the size of the chain [16] $S_L^{xy} = \frac{1}{6}\log_2 L + a(\gamma)$ with a a constant independent of L. Otherwise, it saturates as $S_L \to S_L^*$ for $L \approx \xi$ in the non-critical region. Away from criticality the saturation value S_L^* decreases with decreasing the correlation length. In Fig. 26 we observe that the points corresponding to $L \geqslant 3000$ are only present in the right side of the graph, since points closer to criticality did not fall inside the collapsing curve for $m = 30$. The reason for this is that for large values of L, we need to get closer to the critical point, which implies to have a big m if a good DMRG performance is desired.

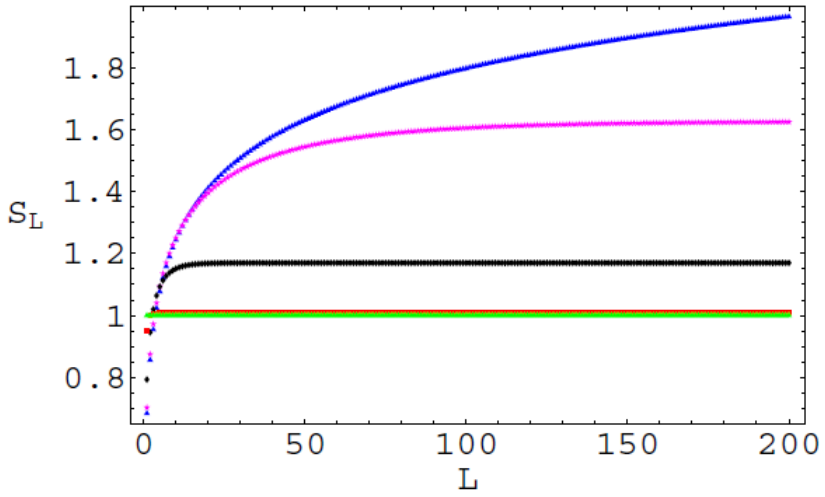

Figure 30: Taken from [16]. Transverse Ising model. Entropy for the reduced density matrix to L spins embedded in an infinite chain. The logarithmic behavior is obtained at the critical point when the magnetic field $\lambda = 1$. Smaller values of λ have a small saturation vlaue for the entropy.

Second important observation is that in Fig. 29, the fluctuations of the collapsing curve are higher than those for $\gamma = 1$ in Fig. 26. We are still looking for a reasonable explanation to this fact since (contrary to our wishes) Fig.31 exposes the fact that for the XY model, entropy should decrease for $\gamma < 1$.

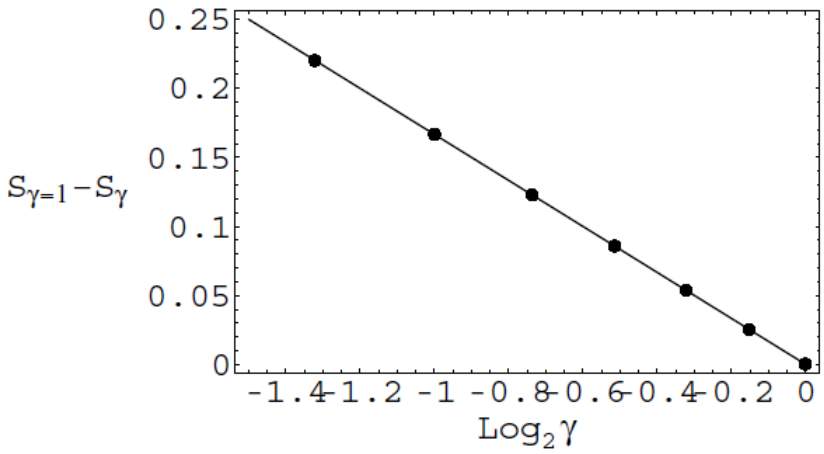

Figure 31: Taken from [16]. Difference of the entropy $\lim_{L\to\infty}[S_L(\gamma = 1) - S_L(\gamma)] = -\frac{1}{6}\log_2\gamma$.

When the perturbed Hamiltonian is considered $B_x \ll B_z$ in Eq. 4.9, the $\mathbb{Z}_2$ symmetry is broken. This model is integrable and it also presents a phase transition

at $J = B_z$ and $B_x = 0$, but belongs to a different universality class and therefore $\nu = 8/15$ and $\beta = 1/15$.

In this case, DMRG method can be used directly since there is no ambiguity in the ground state due to the perturbation field B_x. In Fig. 32 the first 6 Schmidt eigenvalues as a function of B_x/B_z with $B_z = J = 1$ are plotted using the Matlab code presented in Appendix 3. We observed that the Schmidt gap decreases in the limit $B_x \to 0$.

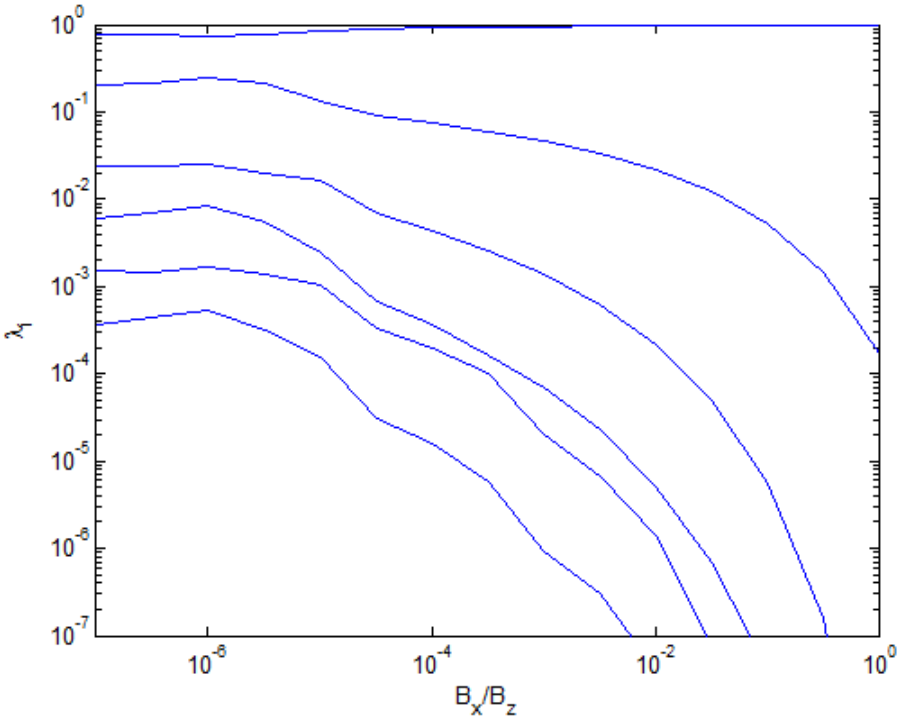

Figure 32: First 6 Schmidt eigenvalues for the Ising model with longitudinal perturbation as a function of B_x/B_z for $L = 384$.

Again,we use the finite size scaling theory and apply Eq. 4.10 with $g = B_x$ and $g_c = 0$. Fig. 33 shows the collapsing curve for different values of L. In this case $\mu_1 = 0.11$ and $\mu_2 = 2$, from where we obtain that $\beta = 0.055$ and $\nu = 0.5$, which again are in good agreement with the corresponding exponents of this phase transition.

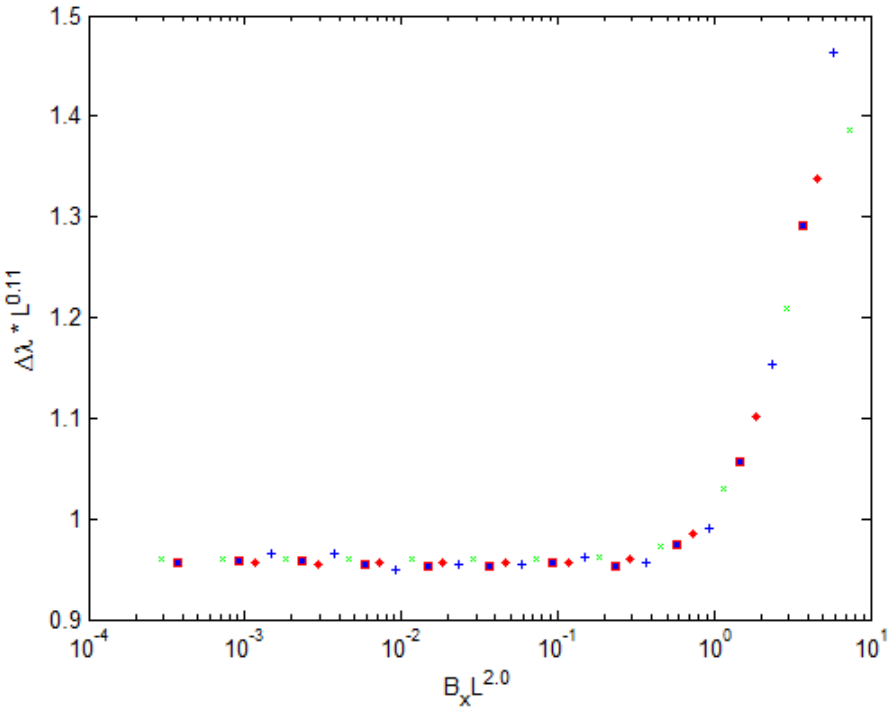

Figure 33: Finite size scaling analysis for the perturbed model, when $B_x \to 0$ for $L = 48, 96, 192, 384$.

Next Chapter we will suggest that it would be worth to look at the behavior of the Schmidt gap or even at the whole spectrum of the reduced density matrix in the border of the ellipse known as the disorder line of the XY model that distinguishes an ordinary ferromagnetic phase from the oscillatory one.

5

GNS CONSTRUCTION AND XY MODEL

In this chapter we follow [2] to apply the new approach of entanglement based on the Gelfand-Naimark-Segal (GNS) construction to the two site XY model. In this approach the conventional idea of taking the partial trace of a bipartite system is replaced by a more general point of view of restricting the state to a subalgebra. The idea was developed in [2] , giving a satisfactory understanding to the generalization of entanglement's measures to non-identical particle systems, a concept that has caused a lot of confusion and contradictory results [26].

5.1 GNS CONSTRUCTION

In quantum mechanics we described a quantum system by establishing the Hilbert space, the space of states, and a set of self-adjoint operators $(\mathcal{O} \equiv \mathcal{O}^\dagger : \mathcal{H} \to \mathcal{H})$ acting on it. More general, states are described by density matrices $\rho : \mathcal{H} \to \mathcal{H}$, which are linear maps satisfying $\mathrm{Tr}(\rho) = 1$ (normalization), $\rho^\dagger = \rho$ (self-adjointness) and $\rho \geqslant 0$ (positivity).

Since the expectation value of an observable $\mathcal{O}$ is given by $\langle \mathcal{O} \rangle = \mathrm{Tr}(\rho\mathcal{O})$, it is also possible to look at the density matrix as a linear functional $\omega_\rho : \mathcal{A} \to \mathbb{C}$ with $\mathcal{A}$ a C*-algebra, the algebra of observables. We assume that $\mathcal{A}$ is a unitary algebra i.e it contains an identity $\mathbb{1}_\mathcal{A}$. From the properties of normalization, reality and positivity of ρ we have:

$$\omega(\mathbb{1}_\mathcal{A}) = \mathrm{Tr}(\rho) = 1 \qquad \omega(\alpha^*) = \overline{\omega(\alpha)} \qquad \omega(\alpha^*\alpha) \geqslant 0, \tag{5.1}$$

for $\alpha \in \mathcal{A}$. The last property can be easily checked by calculating $\mathrm{Tr}(\alpha^*\alpha\rho)$ in the diagonal basis of ρ , regarding that the trace is invariant under change of basis.

In the light of the above, if we start with an algebra of observables $\mathcal{A}$ and a linear functional ω which satisfies Eq.5.1, the GNS construction allows us to construct the Hilbert space on which the algebra acts on. The requirement of $\mathcal{A}$ to be a C*-algebra, guarantees that these properties can be fulfilled without having yet constructed the Hilbert space. This is because a C*-algebra is a complete normed algebra $(\mathcal{A}, \|.\|)$, with an antilinear involution $\alpha \to \alpha^*$, such that $\|\alpha^*\alpha\| = \|\alpha^2\|$ for all $\alpha \in \mathcal{A}$ is satisfied.

The construction of the Hilbert space goes as follows: Since $\mathcal{A}$ is an algebra it is also a vector space, let us denote $|\alpha\rangle$ the elements on this vector space. Therefore, the algebra can act on itself using the product operation of the algebra. In order to become this vector space a Hilbert space we need to endow it with an inner product, hence the first try would be $\langle\alpha|\beta\rangle = \omega(\alpha^*\beta)$ for α, β in $\mathcal{A}$. The linearity condition is given by the linearity of the functional ω, the conjugate symmetry axiom $\langle\beta|\alpha\rangle = \overline{\langle\alpha|\beta\rangle}$ comes from Eq.5.1 because $\omega((\alpha^*\beta)^*) = \omega(\beta^*\alpha) = \overline{\omega(\alpha^*\beta)}$ and $\langle\alpha|\alpha\rangle \geqslant 0$ is given by positivity. However, it is still possible to have $\langle\alpha|\alpha\rangle = 0$ for non-zero elements α. We can take the quotient space $\mathcal{A}/\mathcal{N}_\omega$, with $\mathcal{N}_\omega = \{\,|\alpha\rangle \in \mathcal{A} \,|\, \omega(\alpha^*\alpha) = 0\,\}$ to solve the problem.

The elements of $\mathcal{A}/\mathcal{N}_\omega$ are equivalence classes that we denote $|[\alpha]\rangle$, where $[\alpha] = \alpha + \mathcal{N}_\omega$. Using Schwarz inequality ($|\langle x|y\rangle|^2 \leqslant \langle x|x\rangle\langle y|y\rangle$), we can show that $a\mathcal{N}_\omega \subseteq \mathcal{N}_\omega$ and $\langle a|\alpha\rangle = 0$ for all $a \in \mathcal{A}$, $\alpha \in \mathcal{N}_\omega$:

- Consider $a\alpha$ such that $a \in \mathcal{A}$, $\alpha \in \mathcal{N}_\omega$, then $\langle a\alpha|a\alpha\rangle = \omega(\alpha^*a^*a\alpha) = \langle\alpha|a^*a\alpha\rangle \leqslant \sqrt{\langle\alpha|\alpha\rangle\langle a^*a\alpha|a^*a\alpha\rangle} = 0$, since $\langle\alpha|\alpha\rangle = 0$, then $a\alpha \in \mathcal{N}_\omega$.
- $|\langle a|\alpha\rangle|^2 \leqslant \langle a|a\rangle\langle\alpha|\alpha\rangle = 0$, then $\langle a|\alpha\rangle = 0$

Now, we are ready to define an inner product on $\mathcal{A}/\mathcal{N}_\omega$:

$$\langle[\alpha]|[\beta]\rangle = \omega(\alpha^*\beta), \tag{5.2}$$

it has no nontrivial null vectors and from the properties shown above it does not depend on the choice of β from $[\beta]$. To see this take $\beta' = \beta + n$ with $n \in \mathcal{N}_\omega$, then $\langle[\alpha]|[\beta']\rangle = \langle\alpha|\beta\rangle + \langle\alpha|n\rangle = \langle\alpha|\beta\rangle$.

The closure of $\mathcal{A}/\mathcal{N}_\omega$ is the GNS Hilbert space $\mathcal{H}_\omega$, notice that it depends on the algebra and the state ω. At this point, $\mathcal{A}$ can act on $\mathcal{H}_\omega$ through a representation denoted as π_ω, such that $\pi_\omega(\alpha)|[\beta]\rangle = |[\alpha\beta]\rangle$. This representation is well defined:

Take $\beta' = \beta + n$, then $\pi_\omega(\alpha)|[\beta']\rangle = |[\alpha\beta']\rangle$. Since $\alpha\beta - \alpha\beta' = -\alpha n$ and $\alpha n \in \mathcal{N}_\omega$ we have $|[\alpha\beta']\rangle = |[\alpha\beta]\rangle$.

The representation π_ω is in general reducible, therefore we can decompose $\mathcal{H}_\omega$ into irreducible spaces $\mathcal{H}_\omega = \oplus_i \mathcal{H}_i$ and we can define the projectors $P_i : \mathcal{H}_\omega \to \mathcal{H}_i$ that satisfy the orthogonal relation $P_iP_j = P_j\delta_{ij}$.

We use these projectors to create a density matrix ρ_ω in $\mathcal{H}_\omega$ that reproduces the same expectation values as ω. We define $\rho_\omega = \sum_i P_i|[\mathbb{1}_\mathcal{A}]\rangle\langle[\mathbb{1}_\mathcal{A}]|P_i$ and propose $\omega(\alpha) = \mathrm{Tr}_{\mathcal{H}_\omega}(\rho_\omega\pi_\omega(\alpha))$. Let us prove the last assertion, consider $\{|[m]\rangle\}$ an orthonormal basis of $\mathcal{H}_\omega$, then:

$$\begin{aligned}\mathrm{Tr}_{\mathcal{H}_\omega}(\rho_\omega \pi_\omega(\alpha)) &= \sum_{i,m} \langle [m]|\, P_i\, |[\mathbb{1}_{\mathcal{A}}]\rangle \langle [\mathbb{1}_{\mathcal{A}}]|\, P_i\, \pi_\omega(\alpha)|[m]\rangle \\ &= \sum_i \langle [\mathbb{1}_{\mathcal{A}}]|\, P_i\, \pi_\omega(\alpha)\, P_i\, |[\mathbb{1}_{\mathcal{A}}]\rangle \end{aligned} \tag{5.3}$$

On the other hand, for every vector $|[v]\rangle \in \mathcal{H}_\omega$ we have $|[v]\rangle = \sum_i P_i|[v]\rangle$ and using the fact that $\mathcal{H}_i$ is an invariant subspace of the representation we obtain:

$$\langle [v]|\pi_\omega(\alpha)|[v]\rangle = \sum_{i,j} \langle [v]|\, P_i\, \pi_\omega(\alpha)\, P_j\, |[v]\rangle = \sum_i \langle [v]|\, P_i\, \pi_\omega(\alpha)\, P_i\, |[v]\rangle, \tag{5.4}$$

in particular we have $\sum_i \langle [\mathbb{1}_{\mathcal{A}}]|\, P_i\, \pi_\omega(\alpha)\, P_i\, |[\mathbb{1}_{\mathcal{A}}]\rangle = \langle [\mathbb{1}_{\mathcal{A}}]|\pi_\omega(\alpha)|[\mathbb{1}_{\mathcal{A}}]\rangle = \langle [\mathbb{1}_{\mathcal{A}}]|[\alpha]\rangle = \omega(\alpha)$ and from Eq5.3 we obtain the desire result:

$$\omega(\alpha) = \mathrm{Tr}_{\mathcal{H}_\omega}(\rho_\omega \pi_\omega(\alpha)). \tag{5.5}$$

We can also define the following othonormal vectors:

$$|[\chi_i]\rangle = (1/\sqrt{\mu_i})\, P_i\, |[\mathbb{1}_{\mathcal{A}}]\rangle \qquad \text{with} \qquad \mu_i = \| P_i\, |[\mathbb{1}_{\mathcal{A}}]\rangle\|^2, \tag{5.6}$$

they satisfy $\langle [\chi_i]|[\chi_i]\rangle = \delta_{ij}$ and regarding the expression for ρ_ω given before, we obtain:

$$\rho_\omega = \sum_i \mu_i\, |[\chi_i]\rangle\, \langle [\chi_i]| \tag{5.7}$$

Therefore, the von Neumann entropy associated to ρ_ω is given by $S(\rho_\omega) = -\mathrm{Tr}_{\mathcal{H}_\omega}(\rho_\omega \log \rho_\omega) = -\sum_i \mu_i \log \mu_i$ and it can be seen as the expectation value of the operator $\log \rho_\omega$. As a result, ω is pure if and only if the representation is irreducible, in which case $S = 0$.

5.1.1 *Important Note:*

The element $|[\mathbb{1}_{\mathcal{A}}]\rangle$ is cyclic with respect to $\pi_\omega(\mathcal{A})$, since $\pi_\omega(\mathcal{A})|[\mathbb{1}_{\mathcal{A}}]\rangle$ is dense in $\mathcal{H}_\omega$. In this sense a state identifies a family of states to which it is related with and it is possible to look at $\mathcal{H}_\omega$ like the "phase" or close world to which ω belongs.

An interesting question is then, how many closed worlds does a physical system has. In [24] and [15] it is explain that different phases correspond to inequivalent

representation of $\mathcal{A}$ and states in $\mathcal{H}_\omega$ define unitary equivalent representations of $\mathcal{A}$.

For systems of finite degrees of freedom there is only one representation up to unitary equivalence and therefore only one phase is possible. This is why QPT are only possible in the thermodynamic limit.

5.2 PARTIAL TRACE AS RESTRICTION

Consider a bipartite system with a Hilbert space given by $\mathcal{H} = \mathcal{H}_A \otimes \mathcal{H}_B$ our aim is to study the entanglement between both parts of the system from the GNS construction point of view. Here we still follow [2]. We now focus on the operators acting only on subsystem A, that is, in the subalgebra $\mathcal{A}_o$ of local operators of the form $K \otimes \mathbb{1}_B$, for K observable on $\mathcal{H}_A$. We can define a state $\omega_{\rho,o} : \mathcal{A}_o \to \mathbb{C}$ to be the restriction of ω_o to $\mathcal{A}_o$ i.e $\omega_{\rho,o}(\alpha) = \omega(\alpha)$ for $\alpha = K \otimes \mathbb{1}_B \in \mathcal{A}_o$. Regarding that for a bipartite system we have $Tr_{\mathcal{H}}(\alpha\rho) = Tr_{\mathcal{H}_A}(\rho_A K)$, then:

$$\omega_{\rho,o}(K \otimes \mathbb{1}_B) = Tr_{\mathcal{H}_A}(\rho_A K), \tag{5.8}$$

consequently we can perform the GNS construction restricted to the algebra $\mathcal{H}_A$ and $\omega_{\rho,o}$.

Example: In order to illustrate this, let us assume we have a two particle system of spin 1/2 in the state $|\psi_\lambda\rangle = \sqrt{\lambda}|+,-\rangle + \sqrt{(1-\lambda)}|-,+\rangle$. Since $\rho_A = Tr_B(|\psi_\lambda\rangle\langle\psi_\lambda|)$ we have:

$$\rho_A = \begin{pmatrix} \lambda & 0 \\ 0 & 1-\lambda \end{pmatrix}, \tag{5.9}$$

therefore, the entanglement entropy is given by,

$$S(\rho_A) = -\lambda \log \lambda - (1-\lambda)\log(1-\lambda). \tag{5.10}$$

For $0 < \lambda < 1$ the state is entangled, for $\lambda = 0, 1$ we have a product state. Let us analyze these cases separately in order to perform the GNS construction. The total algebra for this system is given by $\mathcal{A} = M_2(\mathbb{C}) \otimes M_2(\mathbb{C})$ and the subalgebra restricted to the first site would be $\mathcal{A}_o \cong M_2(\mathbb{C})$. The restricted functional is obtain as follows:

$$\begin{aligned}\omega_o(\beta \otimes \mathbb{1}_{\mathcal{B}}) &= \langle \psi_\lambda || \beta \otimes \mathbb{1}_{\mathcal{B}} || \psi_\lambda \rangle \\ &= \lambda \langle + |\beta| + \rangle + (1-\lambda)\langle - |\beta| - \rangle \\ &= \lambda\beta_{11} + (1-\lambda)\beta_{22} \equiv \omega_o(\beta) \end{aligned} \tag{5.11}$$

Case: $0 < \lambda < 1$.

First we need to find the null space $\mathcal{N}_\omega$, using Eq.5.11 we calculate $\omega_o(\beta^*\beta) = 0$ and obtain the following condition:

$$\lambda(|\beta_{11}|^2 + |\beta_{21}|^2) + (1-\lambda)(|\beta_{12}|^2 + |\beta_{22}|^2) = 0. \tag{5.12}$$

In this case the solution to this equation is $\beta = 0$ implying that $\mathcal{N}_\omega = \{0\}$. This means that $\mathcal{H}_\omega \cong \mathbb{C}^4$ and we can consider the 2×2 matrices $e_{i,j}$ with a 1 in its (i,j) entry and zeros elsewhere as a basis of the Hilbert space. It is easy to show that in the following order basis $\{\,|[e_{11}]\rangle, |[e_{21}]\rangle, |[e_{12}]\rangle, |[e_{22}]\rangle\,\}$ we can express:

$$\pi_{\omega_o}(\beta) = \begin{pmatrix} \beta & 0 \\ 0 & \beta \end{pmatrix}, \tag{5.13}$$

for any $\beta \in \mathcal{A}_o$. From Eq. 5.13 we observe that the representation π_{ω_o} is irreducible and it has as invariant subspaces $\mathcal{H}_1$ spanned by $\{|[e_{11}]\rangle, |[e_{21}]\rangle\}$ and $\mathcal{H}_2$ spanned by $\{|[e_{12}]\rangle, |[e_{22}]\rangle\}$, in addition the identity vector is decomposed into these subspaces as follows:

$$|\mathbb{1}_{\mathcal{A}}\rangle = |[e_{11}]\rangle + |[e_{22}]\rangle. \tag{5.14}$$

From Eq.5.6 we see that $\mu_1 = \langle [\mathbb{1}_{\mathcal{A}}]|\, P_1 P_1\, |[\mathbb{1}_{\mathcal{A}}]\rangle = \lambda$, similarly $\mu_2 = 1-\lambda$ and now, using Eq.5.7 we find the expression for the GNS entropy:

$$S(\omega_o) = -\lambda \log \lambda - (1-\lambda)\log(1-\lambda), \tag{5.15}$$

which is precisely the entropy of the reduced density matrix ρ_A obtain in Eq.5.10.

Case: $\lambda = 0$

The expression Eq.5.12 is valid for $\lambda = 0, 1$ as well, consequently we see that $\mathcal{N}_\omega \cong \mathbb{C}^2$ and it is spanned by elements of the form:

$$\beta = \begin{pmatrix} \beta_{11} & 0 \\ \beta_{21} & 0 \end{pmatrix}. \tag{5.16}$$

Hence, $\mathcal{H}_{\omega_o} = \mathcal{A}/\mathcal{N}_{\omega_o} \cong \mathbb{C}^2$ and is generated by $|[e_{12}]\rangle$ and $|[e_{22}]\rangle$. In this case the representation is irreducible, moreover, the identity vector can be expressed:

$$|[\mathbb{1}_{\mathcal{A}}]\rangle = |[e_{22}]\rangle, \tag{5.17}$$

showing that $\mu_1 = 1$ and $S(\omega_0) = 0$. This result also agrees with Eq.5.10. A very similar procedure is follow for $\lambda = 0$, showing also that $S(\omega_0) = 0$.

The results just obtained, are indeed general for bipartite systems: [2] "*For bipartite systems of the form $\mathcal{H}_A \otimes \mathcal{H}_B$(pure case), the GNS construction yields a vanishing entropy for the restricted state precisely when the original state of the full-system is separable. Moreover, in the case of entangle states, the entropy computed via GNS construction coincides with the von Neumann entropy of the reduced density matrix computed via partial trace and can therefore be used as an entanglement measurement.*"

5.3 GNS CONSTRUCTION APPLIED TO THE TWO SITE XY MODEL

We have already implemented the GNS construction restricted to a local subalgebra $\mathcal{A}_o$ to study the entanglement of bipartite systems. Many other possibilities can be explored by performing the GNS construction restricted to different subalgebras, the aim is to physically interpret the meaning of what we defined by the GNS entanglement expression.

Here we study the two site XY model and give the first step towards the implementation of the GNS construction restricted to the subalgebra that we called the *Even algebra*. We analyze the dimension of the GNS Hilbert space corresponding to the ground state for different regions in the space of parameters that determines the system's Hamiltonian.

The Hamiltonian that describes the system under consideration is:

$$H(B_z, \gamma) = (\frac{1+\gamma}{2})\sigma_x \otimes \sigma_x + (\frac{1-\gamma}{2})\sigma_y \otimes \sigma_y + \frac{B_z}{2}\mathbb{1} \otimes \sigma_z + \frac{B_z}{2}\sigma_z \otimes \mathbb{1}. \tag{5.18}$$

In the following order basis $\{|+,+\rangle, |+,-\rangle, |-,+\rangle, |-,-\rangle\}$,notice that we have change $B_z \to B_z/2$ with respect to the notation used in Chapter 4. This Hamiltonian takes the matrix form:

$$H = \begin{pmatrix} B_z & 0 & 0 & \gamma \\ 0 & 0 & 1 & 0 \\ 0 & 1 & 0 & 0 \\ \gamma & 0 & 0 & -B_z \end{pmatrix}, \tag{5.19}$$

The diagonalization can be made by considering the two Hamilontians $H_1 = \begin{pmatrix} B_z & \gamma \\ \gamma & -B_z \end{pmatrix}$ and $H_2 = \begin{pmatrix} 0 & 1 \\ 1 & 0 \end{pmatrix}$ defined on the subspaces spanned by $\{|+,+\rangle, |-,-\rangle\}$ and $\{|+,-\rangle, |-,+\rangle\}$ respectively. Consequently, the eigenvalues and eigenvectors of the two matrices are:

$$
\begin{aligned}
E^1_\pm &= \pm\sqrt{B_z^2+\gamma^2}, \\
|E^1_+\rangle &= \cos\frac{\alpha}{2}|+,+\rangle + \sin\frac{\alpha}{2}|-,-\rangle, \\
|E^1_-\rangle &= -\sin\frac{\alpha}{2}|+,+\rangle + \cos\frac{\alpha}{2}|-,-\rangle, \\
E^2_\pm &= \pm 1, \\
|E^2_+\rangle &= \frac{1}{\sqrt{2}}(|+,-\rangle + |-,+\rangle), \\
|E^2_-\rangle &= \frac{1}{\sqrt{2}}(|-,+\rangle - |+,-\rangle),
\end{aligned}
\tag{5.20}
$$

with $\tan\alpha = \dfrac{\gamma}{B_z}$ and $\tan\alpha/2 = \tan\alpha/(1+\sqrt{1+\tan^2\alpha})$, $0 \leqslant \alpha \leqslant \dfrac{\pi}{2}$. As shown if Fig.34 for $B_z^2+\gamma^2 > 1$ the ground state of the system is $|E^1_-\rangle$, while for $B_z^2+\gamma^2 < 1$ the ground state is given by $|E^2_-\rangle$. Over the curve of unitary radio the ground state is degenerated by both states.

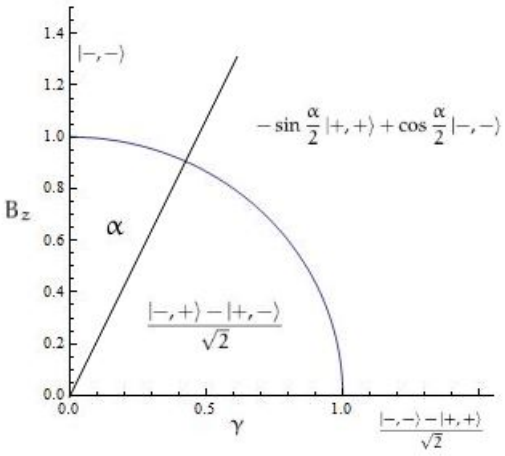

Figure 34: Ground states of the two site XY model for different values of B_z and γ

Notice that the Hamiltonian Eq.5.18 is invariant under the $\mathbb{Z}_2$ symmetry $\sigma_z \to \sigma_z$, $\sigma_x \to -\sigma_x$ and $\sigma_y \to -\sigma_y$, which can be implemented on total algebra by the following inner automorphism:

$$\begin{aligned} P : M_2(\mathbb{C}) \otimes M_2(\mathbb{C}) &\to M_2(\mathbb{C}) \otimes M_2(\mathbb{C}) \\ \alpha \quad \otimes \quad \beta \quad &\to \sigma_z \alpha \sigma_z \otimes \sigma_z \beta \sigma_z \end{aligned} \tag{5.21}$$

Now we define the *Even algebra* $\mathcal{A}_+ = \{ \alpha \otimes \beta \in M_2(\mathbb{C}) \otimes M_2(\mathbb{C}) \,|\, P(\alpha \otimes \beta) = \alpha \otimes \beta \}$. Regarding that the elements of the form $\sigma_i \otimes \sigma_j$ for $i, j = 1, 2, 3, 4$ corresponding to the three Pauli matrices and the identity formed a basis of the total algebra, it is easy to check that the *Even algebra* is spanned by Eq.5.22, where the matrices are expressed in the following order eigenbasis $\Omega = \{ |E^1_-\rangle, |E^2_-\rangle, |E^1_+\rangle, |E^2_+\rangle \}$:

$$\mathbb{1} \otimes \mathbb{1} = \begin{pmatrix} 1 & 0 & 0 & 0 \\ 0 & 1 & 0 & 0 \\ 0 & 0 & 1 & 0 \\ 0 & 0 & 0 & 1 \end{pmatrix}, \quad \mathbb{1} \otimes \sigma_z = \begin{pmatrix} -\cos\alpha & 0 & -\sin\alpha & 0 \\ 0 & 0 & 0 & 1 \\ -\sin\alpha & 0 & \cos\alpha & 0 \\ 0 & 1 & 0 & 0 \end{pmatrix}, \quad \sigma_z \otimes \mathbb{1} = \begin{pmatrix} -\cos\alpha & 0 & -\sin\alpha & 0 \\ 0 & 0 & 0 & -1 \\ -\sin\alpha & 0 & \cos\alpha & 0 \\ 0 & -1 & 0 & 0 \end{pmatrix},$$

$$\sigma_z \otimes \sigma_z = \begin{pmatrix} 1 & 0 & 0 & 0 \\ 0 & -1 & 0 & 0 \\ 0 & 0 & 1 & 0 \\ 0 & 0 & 0 & -1 \end{pmatrix}, \quad \sigma_x \otimes \sigma_x = \begin{pmatrix} -\sin\alpha & 0 & \cos\alpha & 0 \\ 0 & -1 & 0 & 0 \\ \cos\alpha & 0 & \sin\alpha & 0 \\ 0 & 0 & 0 & 1 \end{pmatrix}, \quad \sigma_x \otimes \sigma_y = \begin{pmatrix} 0 & 0 & i & 0 \\ 0 & 0 & 0 & -i \\ -i & 0 & 0 & 0 \\ 0 & i & 0 & 0 \end{pmatrix},$$

$$\sigma_y \otimes \sigma_x = \begin{pmatrix} 0 & 0 & i & 0 \\ 0 & 0 & 0 & i \\ -i & 0 & 0 & 0 \\ 0 & -i & 0 & 0 \end{pmatrix}, \quad \sigma_y \otimes \sigma_y = \begin{pmatrix} \sin\alpha & 0 & -\cos\alpha & 0 \\ 0 & -1 & 0 & 0 \\ -\cos\alpha & 0 & -\sin\alpha & 0 \\ 0 & 0 & 0 & 1 \end{pmatrix}. \tag{5.22}$$

Our aim is to develop the GNS Hilbert space for the subalgebra $\mathcal{A}_+$ and every ground state illustrated in Fig.34. In general, let us consider the density matrix of Eq. 5.23

$$\rho_\varepsilon = \varepsilon |E^1_-\rangle\langle E^1_-| + (1-\varepsilon)|E^2_-\rangle\langle E^2_-|, \tag{5.23}$$

and the functional,

$$\omega_\varepsilon(a) = \mathrm{Tr}(\rho_\varepsilon a), \qquad \text{for} \quad a \in \mathcal{A}_+. \tag{5.24}$$

Notice that when $\varepsilon = 1 \setminus 0$ we are describing the ground state of the regions outside\inside the unitary circle and when $0 < \varepsilon < 1$ we refer to any possible mixed state that could describe the fundamental state along the border of the circumference. Let us analyze the GNS construction for each case:

Case $\varepsilon = 1$:

From Eq. 5.23 we have $\rho_{\varepsilon=1} = |E^1_-\rangle\langle E^1_-|$. In order to find the null space corresponding to the subalgebra $\mathcal{A}_+$, first we characterize the null space $\mathcal{N}^{\mathcal{A}}_{\omega_{\varepsilon=1}}$ of the total algebra $\mathcal{A} \cong M_2(\mathbb{C}) \otimes M_2(\mathbb{C})$, then we perform the restriction of the space $\mathcal{N}^{\mathcal{A}}_{\omega_{\varepsilon=1}}$ to $\mathcal{A}_+$ so that we end up with the null space $\mathcal{N}^{\mathcal{A}_+}_{\omega_{\varepsilon=1}}$.

Any $\eta \in \mathcal{A}$ can be represented as a 4×4 matrix with entries η_{ij}, when expressed in the order basis $\{|E^1_-\rangle, |E^2_-\rangle, |E^1_+\rangle, |E^2_+\rangle\}$. The null space $\mathcal{N}^{\mathcal{A}}_{\omega_{\varepsilon=1}}$ is calculated by the following condition:

$$\omega_{\varepsilon=1}(\eta^\dagger\eta) = Tr(\rho_{\varepsilon=1}\eta^\dagger\eta) = \langle E^1_-|\eta^\dagger\eta|E^1_-\rangle = |\eta_{11}|^2 + |\eta_{21}|^2 + |\eta_{31}|^2 + |\eta_{41}|^2 = 0, \tag{5.25}$$

this means that $\eta \in \mathcal{N}^{\mathcal{A}}_{\omega_{\varepsilon=1}}$ if it is of the form $\begin{pmatrix} 0 & \eta_{12} & \eta_{13} & \eta_{14} \\ 0 & \eta_{22} & \eta_{23} & \eta_{24} \\ 0 & \eta_{32} & \eta_{33} & \eta_{34} \\ 0 & \eta_{42} & \eta_{43} & \eta_{44} \end{pmatrix}$. The set of 4×4 matrices F_{ij} $(i=1,2,3,4, j=2,3,4)$ with a one in the entry (i,j) and zero elsewhere, forms a basis for $\mathcal{N}^{\mathcal{A}}_{\omega_{\varepsilon=1}}$, which is of dimension 12. Notice that 6 of these matrices can be expand as linear combinations of $\mathcal{A}_+$, for instance, from Eq.5.22:

$$\begin{pmatrix} 0 & 0 & 0 & 0 \\ 0 & 1 & 0 & 0 \\ 0 & 0 & 0 & 0 \\ 0 & 0 & 0 & 0 \end{pmatrix} = \frac{1}{4}(\mathbb{1}\otimes\mathbb{1} - \sigma_z\otimes\sigma_z - \sigma_x\otimes\sigma_x - \sigma_y\otimes\sigma_y), \tag{5.26}$$

These 6 matrices form a basis for $\mathcal{N}^{\mathcal{A}_+}_{\omega_{\varepsilon=1}}$ and we conclude that $\dim(\mathcal{N}^{\mathcal{A}_+}_{\omega_{\varepsilon=1}}) = 6$. Furthermore, since $\mathcal{H}^{\mathcal{A}_+}_{\omega_{\varepsilon=1}} = \mathcal{A}_+/\mathcal{N}^{\mathcal{A}_+}_{\omega_{\varepsilon=1}}$, the dimension of this Hilbert space is $\dim(\mathcal{H}^{\mathcal{A}_+}_{\omega_{\varepsilon=1}}) = 2$.

The matrices F_{ij} with $j=1$ and $i=1,2,3,4$ form a basis of the complement of $\mathcal{N}^{\mathcal{A}}_{\omega_{\varepsilon=1}}$ in $\mathcal{A}$. Two of them F_{11} and F_{31} can be expanded by the basis elements of $\mathcal{A}_+$, see Eq. 5.22, forming the equivalence classes of the basis vectors in $\mathcal{H}^{\mathcal{A}_+}_{\omega_{\varepsilon=1}}$.

Our next argument shows that the GNS representation of $\mathcal{A}_+$ into the two dimensional vector space $\mathcal{H}^{\mathcal{A}_+}_{\omega_{\varepsilon=1}}$ is irreducible, letting us to the conclusion that the GNS entanglement entropy vanishes i.e $S(\omega_{\varepsilon=1}) = 0$.

The argument is based on the fact that for a representation π of an algebra acting on a two dimensional vector space to be reducible, all the 2×2 matrices $\pi(\alpha)$, with $\alpha\in\mathcal{A}$ must be diagonal in the same basis. In general, this condition is very hard to satisfy, in our case, let us define $|[v_1]\rangle \equiv |[F_{11}]\rangle$ and $|[v_2]\rangle \equiv |[F_{31}]\rangle$ as a basis for $\mathcal{H}^{\mathcal{A}_+}_{\omega_{\varepsilon=1}}$, we use them to expressed the matrix representation of the elements $\mathbb{1}\otimes\mathbb{1}$ and $\sigma_x\otimes\sigma_x$:

$$\pi(\mathbb{1}\otimes\mathbb{1}) = \begin{pmatrix} 1 & 0 \\ 0 & 1 \end{pmatrix} \qquad \text{and} \qquad \pi(\sigma_x\otimes\sigma_x) = \begin{pmatrix} 0 & i \\ -i & 0 \end{pmatrix}, \tag{5.27}$$

meaning that the GNS representation is irreducible.

Case $\varepsilon = 0$:

The density matrix is given by $\rho_{\omega_{\varepsilon=0}} = |E^2_-\rangle\langle E^2_-|$, which corresponds to the ground state inside the unitary circle of Fig. 34. A very similar procedure to the one followed for the $\varepsilon = 1$ case shows that the matrices in the null space $\mathcal{N}^{\mathcal{A}}_{\omega_{\varepsilon=0}}$ are of the form $\begin{pmatrix} \eta_{11} & 0 & \eta_{13} & \eta_{14} \\ \eta_{21} & 0 & \eta_{23} & \eta_{24} \\ \eta_{31} & 0 & \eta_{33} & \eta_{34} \\ \eta_{41} & 0 & \eta_{43} & \eta_{44} \end{pmatrix}$. Again we find that 6 matrices from the canonical basis set of $\mathcal{N}^{\mathcal{A}}_{\omega_{\varepsilon=0}}$, can be expanded as linear combinations of elements in $\mathcal{A}_+$, see Eq.5.22.

The result is that $\dim(\mathcal{N}^{\mathcal{A}_+}_{\omega_{\varepsilon=0}}) = 6$ and therefore, $\dim(\mathcal{H}^{\mathcal{A}_+}_{\omega_{\varepsilon=0}}) = 2$ as well.

A very similar calculation to the one develop for $\varepsilon = 1$, shows us that in this case the GNS representation is also irreducible and therefore, the GNS entropy also vanishes.

Case $0 < \varepsilon < 1$:

Here, the density matrix $\rho_\varepsilon = \varepsilon|E^1_-\rangle\langle E^1_-| + (1-\varepsilon)|E^2_-\rangle\langle E^2_-|$ describes any possible mixed state over the border of the circumference, see Fig.34. The condition to obtain the null space of the total algebra is given by:

$$\begin{aligned} \omega_\varepsilon(\eta^\dagger\eta) &= \mathrm{Tr}(\rho_\varepsilon\eta^\dagger\eta) = \varepsilon\,\langle E^1_-|\eta^\dagger\eta|E^1_-\rangle + (1-\varepsilon)\,\langle E^2_-|\eta^\dagger\eta|E^2_-\rangle \\ &= \varepsilon\,(|\eta_{11}|^2 + |\eta_{21}|^2 + |\eta_{31}|^2 + |\eta_{41}|^2) + (1-\varepsilon)\,(|\eta_{12}|^2 + |\eta_{22}|^2 + |\eta_{32}|^2 + |\eta_{42}|^2) = 0, \end{aligned} \tag{5.28}$$

which means that $\eta \in \mathcal{N}^{\mathcal{A}}_{\omega_\varepsilon}$ if and only if η is of the form $\begin{pmatrix} 0 & 0 & \eta_{13} & \eta_{14} \\ 0 & 0 & \eta_{23} & \eta_{24} \\ 0 & 0 & \eta_{33} & \eta_{34} \\ 0 & 0 & \eta_{43} & \eta_{44} \end{pmatrix}$. As a result $\dim(\mathcal{N}^{\mathcal{A}}_{\omega_\varepsilon})$=8, and only 4 matrices of the canonical basis set can be expanded in terms of elements in $\mathcal{A}_+$. The dimension of the GNS Hilbert space in this case is $\dim(\mathcal{H}^{\mathcal{A}_+}_{\omega_\varepsilon}) = 4$ and the set $\mathcal{B} = \{|[F_{11}]\rangle, |[F_{31}]\rangle, |[F_{22}]\rangle, |[F_{42}]\rangle\}$ forms an order basis.

From Eq.5.22 it is possible to show that any element $a \in \mathcal{A}_+$ is of the form $\begin{pmatrix} a_{11} & 0 & a_{13} & 0 \\ 0 & a_{22} & 0 & a_{24} \\ a_{31} & 0 & a_{33} & 0 \\ 0 & a_{42} & 0 & a_{44} \end{pmatrix}$ when expressed in the basis $\mathcal{Q}$ and that its matrix representation in the basis $\mathcal{B}$ is given by:

$$\pi(a) = \begin{pmatrix} a_{11} & a_{13} & 0 & 0 \\ a_{31} & a_{33} & 0 & 0 \\ 0 & 0 & a_{22} & a_{24} \\ 0 & 0 & a_{42} & a_{44} \end{pmatrix}. \tag{5.29}$$

This result makes explicit that the GNS representation is reducible and that $\mathcal{H}^{\mathcal{A}_+}_{\omega_\varepsilon} \cong \mathbb{C}^2 \oplus \mathbb{C}^2$. Moreover, the identity matrix can be decomposed as $|[\mathbb{1}_{\mathcal{A}}]\rangle = |[F_{11}]\rangle + |[F_{22}]\rangle$ and regarding Eqs.5.6, 5.7 we have $\mu_1 = \langle[F_{11}]|[F_{11}]\rangle = \varepsilon$ and

$\mu_2 = \langle [F_{22}] | [F_{22}] \rangle = 1 - \varepsilon$. The entropy of the restricted state in this case is different from zero:

$$S(\rho_{\omega_\varepsilon}) = -\varepsilon \log\varepsilon - (1-\varepsilon)\log(1-\varepsilon). \tag{5.30}$$

We have shown that for the two site model the GNS entropy calculated for the ground states of the whole space of parameters restricted to the algebra $\mathcal{A}_+$ always vanishes, except for the circumference line $B_z^2 + \gamma^2 = 1$, see Fig. 34, where a degeneracy is present and we have characterize the state of the system as a mixed state between the two states degenerated. Here, the entropy depends on the parameter ε that determines the density matrix of the mixed state.

At this point it is important to note that despite of the fact that the ground states Eq.5.20 are almost entangle anywhere in the standard way, which in the light of the above means to restrict the GNS construction to the first site local subalgebra; when we change to the *Even Algebra* the states are not entangled in this new sense.

It is important to remark that in the thermodynamic limit the circumference curve pointing the boundary of ground degeneracy in Fig.34 with notation of Eq. 5.18 becomes the ellipse $h = 2\sqrt{(1-\gamma^2)}$. This curve is known as the disordered line of the model and [13] distinguishes a ferromagnetic phase from an oscillatory one. As explained in [11] this lines are lines of constant entropy.

We consider that a very interesting calculation to perform, regarding our results of Chapter 4, would be to study the behavior of the entanglement spectrum of the reduced density matrix when crossing the disordered line. Again using DMRG will facilitate the desired computation to see whether or not the Schmidt gap at this line presents some special critical behavior.

6

CONCLUSIONS AND PERSPECTIVES

In this work we approached the problem of essentially finding the ground state and phase diagram of many body systems which is itself a complicated task since the number of variables needed to describe a state completely grows exponentially with the number of sites. We have deal with this problem by using the numerical approximation methods NRG and DMRG and we have described what we consider are the most important details when start writing the code. We finally take profit of the fact that the code itself allows us to study the properties of the entanglement spectrum of the system very easily. In particular we have follow the idea of [9] to study the properties of the Schmidt gap near the critical points of the XY model with and with out longitudinal perturbation. In first place we have treated the Bose Hubbard model with NRG methods [4] and found better results for the case were $U >> J$, since in the superfluid regime $U << J$ the ground state is given by a superposition of all possible basis states, many of which are discarded during the NRG method.

We also have built the exact numerical solution for the Bose Hubbard model following [34], we exposed some tricky algorithms that facilitates and speed up the development of the numerical computation and that can also be applied in many other generic problems.

With respect to DMRG algorithm we have looked at it's theoretical basis with more care and as an example we have performed the ground state for the infinite antiferromagnetic Heisenberg chain, checking before that the spectrum of the reduced density matrix decays fast enough to justify the implementation of the DMRG algorithm.

One of the most important issues of this work is that we were able to compute numerically the exact solution for the transverse Ising model in order to compare them with the results obtained using DMRG. With DMRG we were able to calculate very easily the Schmidt gap for the transverse Ising model with and with out perturbation. Following [9] we could realize that the Schmidt gap in this particular case behaves as an order parameter of the quantum phase transition. We have done this by performing a Finite Size Scaling analysis were the critical exponents obtained coincide with those of the universality class of the correponding model.

On the other hand we have also performed the analysis for the XY model when $\gamma = 0.5$ and again since this case belongs to the same universality class than the transverse Ising model, we were able to observe that the critical behavior of the Schmidt gap was given by that of an order parameter.

We would like to point out a very interesting way to continue this project, which is to repeat this analysis over the disordered line present in the XY model and try to figure out if the Schmidt gap can also signal this change of oscillatory regime. Finally, the GNS construction has been explained and applied in the two site XY model case. The total algebra is restricted to what we have called the *Even algebra* and we have studied the notion of entanglement entropy under the restriction. The immediate way to go through is to perform the generalization of this problem to the thermodynamic limit so that we can approach to an analytic comprehension of the entanglement properties that lead us to understand the critical Schmidt gap behavior near criticality.

Part I

APPENDIX

A

APPENDIX

A.1 NRG ALGORITHM FOR BOSE HUBBARD MODEL

We present a sketch of the Matlab code used to obtain the results for the NRG algorithm applied to the Bose Hubbard model presented in chapter 2. The algorithm is not exactly the one explain in section 2.2 but the one used by Wilson to approach the Kondo problem. In this variation only one site is added to the block system at each iteration; this presents a computational advantage since many more states can be kept (the truncation number m can be larger) at each iteration because the matrix that has to be diagonalized is not of dimension $m^2 \times m^2$ as before but of dimension $md \times md$ with d the number of states on a single site.

We also need to take into account that in order to study a Bose Hubbard model not only the lattice number of sites but the number of atoms are important. Here, since we followed [4] only systems with equal number of particles and lattice sites are considered; in other words systems with filling factor $\rho = N/I = 1$ with N the number of atoms and I the number of lattice sites.

The following is an explanation of the most important functions developed in the Matlab code used to study the NRG algorithm applied to the Bose Hubbard model and is based completely on reference [4].

Usually the algorithm starts using a two site block and defining a minimum and a maximum number of particles on it. Since the Hamiltonian commutes with the Number of particles operator, this can be expressed as a block diagonal matrix, with each block representing a defined number of particles. The first step is to construct a basis for the block with this range of particle numbers see Fig. 35 for an example.

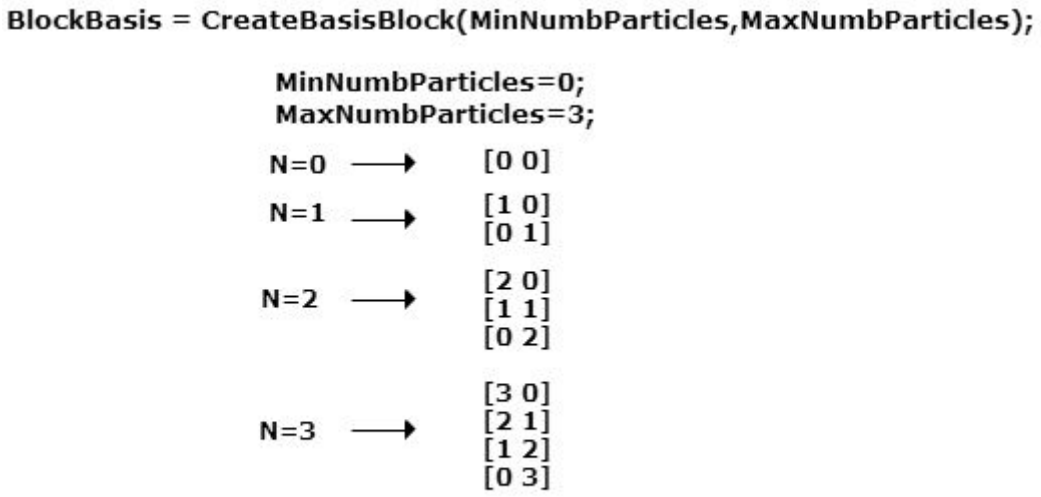

Figure 35: Sketch of what the function CreateBasisBlock does.

Similarly, the basis for the next site to be added is constructed, in this case the atoms are distributed in a single site. The Hamiltonians for the Block and Site systems have to be constructed, the more convenient way is to express the creation and annihilation operators in their respective basis:

$$\begin{aligned} H_B^1 &= -J\{\hat{a}_1^\dagger \hat{a}_2 + \hat{a}_2^\dagger \hat{a}_1\} + \frac{U}{2}\{\hat{n}_1(\hat{n}_1 - 1) + \hat{n}_2(\hat{n}_2 - 1)\} \\ H_S^1 &= \frac{U}{2}\{\hat{n}_3(\hat{n}_3 - 1)\}, \end{aligned} \tag{A.1}$$

with J the hopping term and U the interaction term. For building the Hamiltonian of the three sites "superblock" we need to take into account the following (A.2):

$$\begin{aligned} H_{super}^1 &= \tilde{H}_B^1 + \tilde{H}_S^1 + H_{BS}^1 \\ \tilde{H}_B^1 &= H_B^1 \otimes \mathbb{1}_{d\times d} \\ \tilde{H}_S^1 &= \mathbb{1}_{m\times m} \otimes H_S^1 \\ H_{BS}^1 &= -J\{\hat{a}_2^\dagger \hat{a}_3 + \hat{a}_3^\dagger \hat{a}_2\} \end{aligned} \tag{A.2}$$

The superblock basis is the tensor product of the site and block basis,therefore the super Hamiltonian will be block diagonal but with many more blocks since the range of particle numbers is now $[N_{minSite} + N_{minBlock}, N_{maxSite} + N_{maxBlock}]$. Notice that in order to construct H_{BS}^1, the creation and annihilaton operators of the last block site and the added site must be expressed in the superbasis. The idea is to rotate the superblock Hamiltonian with a truncated basis so that it becomes a

matrix with the same dimension and structure than the block Hamiltonian. In order to get along with this, we need to discard vectors from the superbasis Hamiltonian in two ways:

- Choose which particle number subspaces will be kept for the next iteration. Use the function **CreateTransformationList**.
- Diagonalized this reduced superHamiltonian and discard in each particle number block the eigenstates with the higher eigenvalues, needed to equal the dimension and structure of the block Hamiltonian.

The function **CreateTransormationList** determines the architecture of the program. We already mentioned that the filling factor we are working with is 1, therefore at the end of the algorithm the number of lattice sites must be equal to the last block of particle numbers, this is because we are interested on conserving the maximum number of states with $\rho = 1$ and the last block is the biggest one. Two cases are relevant here:

- $N_{maxBlock}$ = Length of lattice: Maximum number of particles considered in the first iteration equals the lattice size. In this case the sub-spaces of each particle's number are conserved during every iteration. This means that the range of particles under consideration does not change in the process. See Fig 36 for an example with $N = I = 3$.

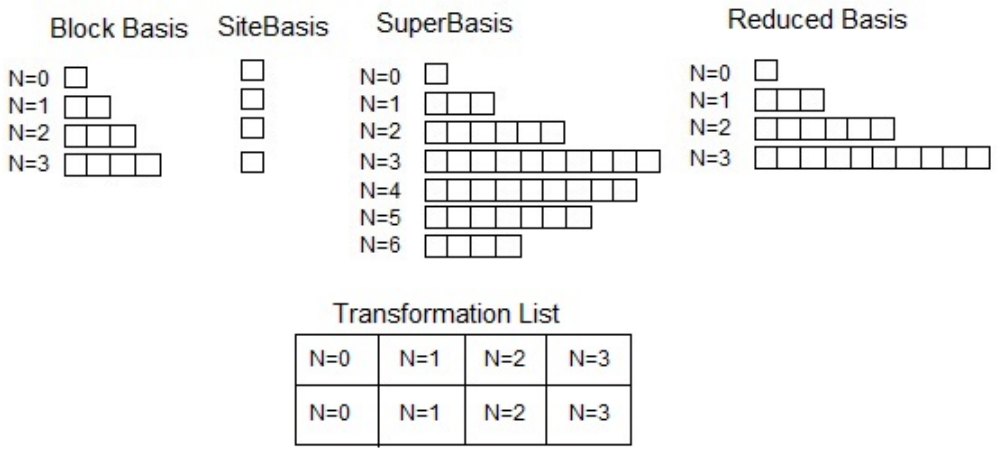

Figure 36: Example:$N_{maxBlock}$ =Length of Lattice= 3. Since only one iteration is needed to get 3 lattice sites Transformation List is just of length 4. It has the information about the correspondence between particle sub-spaces in the block basis and those that result after making the reduction of the super basis.

- $N_{maxBlock}$ < Length of lattice: Maximum number of particles considered in the first iteration is less than the number of lattice sites.In this case the sub-spaces of each particle's number are modified in every iteration in such a way that by the last iteration the biggest particle's number subspace correspond to filling factor 1. See Fig 37

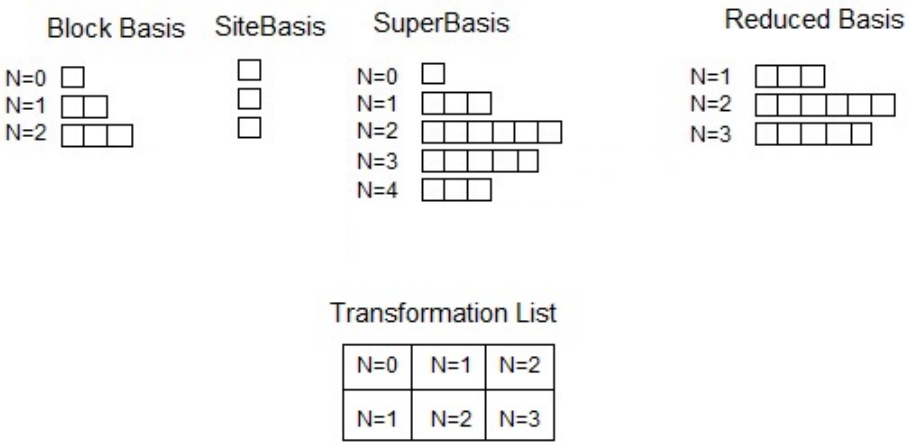

Figure 37: Example:$N_{maxBlock}$ <Length of Lattice= 3. Since only one iteration is needed to get 3 lattice sites Transformation List is just of length 4. Notice that after making the reduction the number of particle assignation to each sub-space increases by 1

Notice that it does not makes sense to keep sub-spaces representing states with $\rho > 1$, because they will not contribute to create the sub-space $\rho = 1$. Therefore, the last block sub-space will always represent states with filling factor less or equal to 1.

We present the part of the code corresponding to the function **CreateTransformationsList**. See Fig 38

```
% Creates a table with the information of the way sub-spaces of the super-Hamiltonian
% are transformed sub-spaces in the block-Hamiltonian of the next iteration
function TransformationsList = CreateTransformationsList(FinalPartNumber, IterationsNumber,
                                        BlockBasisPartNumberMax, BlockBasisPartNumberMin)
%Number of iterations where the correspondence between the block of the
%super-Hamiltonian and the block of the Hamiltonian is changed by 1.
RaisingTransformationsNumber=FinalPartNumber- BlockBasisPartNumberMax;
%Number of iterations where the correspondence between the block of the
%super-Hamiltonian and the block of the Hamiltonian remains.
ConstantTransformationsNumber = IterationsNumber- RaisingTransformationsNumber;
TransformationsList=[];
for j=1:ConstantTransformationsNumber,
    NumberPartBlock=BlockBasisPartNumberMax-BlockBasisPartNumberMin +1;
    for i=1:NumberPartBlock
    Transformation(1,i)= BlockBasisPartNumberMin + i -1;
    Transformation(2,i)= BlockBasisPartNumberMin + i -1;
    end
    TransformationsList=[TransformationsList Transformation];

end

for k=1:RaisingTransformationsNumber,
    NumberPartBlock=BlockBasisPartNumberMax-BlockBasisPartNumberMin +1;
    for l=1:NumberPartBlock
    Transformation(1,l)= BlockBasisPartNumberMin + l -1+ k;
    Transformation(2,l)= BlockBasisPartNumberMin + l -1 + k-1;
    end
    TransformationsList=[TransformationsList Transformation];
end
```

Figure 38: Matlab code corresponding to the function **CreateTransformationsList**

We used the function **OperatorInReducedBasis** to express the superHamiltonian, annihilation and creation operators, in the reduced basis constructed as explain before. Since this basis has not yet been sorted by number of particles, the function **CreatePositionsListAndSortMatrix** produces a transformation matrix M such that $M^{\dagger}H^{1}_{super}M$ is block diagonal. At this point the diagonalization of this block diagonal Hamiltonian can be done by blocks. In Fig.39 the Matlab code for this function **CreateSortetHamiltonEigenSystems** is presented.

```
%This function diagonalizes the SuperBlock-diagonal
%terms.SuperHamiltonEigensystems has the matrices with the eigenvectors and
%eigenvalues of each SuperBlock
function [SuperHamiltonEigenSystem] = CreateSortetHamiltonEigenSystems(SubSpacePartNumber,
                                                                       SortetSuperHamiltonMatrix)
%Number of diagonal blocks each corresponding to a particle´s number.
NumberOfSubSpaces=length(SubSpacePartNumber);
SuperHamiltonEigenSystem= cell(2,NumberOfSubSpaces);
InitialPosition=1;
FinalPosition=0;

for j=1:NumberOfSubSpaces,

    SubspaceDim=SubSpacePartNumber(1,j);
    FinalPosition= FinalPosition+SubSpacePartNumber(1,j);
    SubMatrix= SortetSuperHamiltonMatrix(InitialPosition:FinalPosition, InitialPosition:FinalPosition);
    InitialPosition= InitialPosition+SubSpacePartNumber(1,j);

    [EigenVect,EigenVal] = eig(SubMatrix);

    SuperHamiltonEigenSystem{1,j}=EigenVect;
    SuperHamiltonEigenSystem{2,j}=EigenVal;

end
```

Figure 39: Matlab code corresponding to the function **CreateSortetHamiltonEigenSystems**

It produces the eigenstates and eigenvalues corresponding to each diagonal block of the Reduced Sorted Hamiltonian. With this information we create the matrix transformation that truncates the sorted Reduced Basis by discarding the eigenstates with the higher eigenvalues of each diagonal block. We used the function **Create-TransformationMatrix** to create this matrix that allows us to give the Reduced Hamiltonian the same dimension and structure as the initial block Hamiltonian.

```
%Creates the TransformationMatrix that gives the ReducedBasisHamilton the
%same structure as the BlockHamilton by truncating the greatest
%eigenvectors.
function [TransformationMatrix] = CreateTransformationMatrix(SuperHamiltonEigenSystem,ReducedBasisDim,
                                        BlockBasisDimension,BlockSubSpacePartNumber,SubSpacePartNumber)

TransformationMatrix= zeros(ReducedBasisDim,BlockBasisDimension);
ZerosUp=[];
ZerosDown=zeros(ReducedBasisDim,1);
NumberOfSubSpaces=length(SuperHamiltonEigenSystem);
Column=0;
%Loop for running through each SubBlock
for j=1:NumberOfSubSpaces,
   ZerosDown= ZerosDown(1:(length(ZerosDown)-SubSpacePartNumber(1,j)));
     %sort eigenvalues in descending order
     [SuperHamiltonEigenSystem{2,j} order] = sort(diag(SuperHamiltonEigenSystem{2,j}),'ascend');
      SuperHamiltonEigenSystem{1,j} = SuperHamiltonEigenSystem{1,j}(:,order);

     %P=zeros(SubSpacePartNumber(1,j), 1);
      for k=1:BlockSubSpacePartNumber(1,j),

          TransformationMatrix(:,Column+k)= [ZerosUp; SuperHamiltonEigenSystem{1,j}(:,k); ZerosDown];
          %TransformationMatrix(:,Column+k)= [ZerosUp; P; ZerosDown];

      end

    Column=Column+BlockSubSpacePartNumber(1,j);
    Temp=zeros(SubSpacePartNumber(1,j),1);
    ZerosUp=[ZerosUp; Temp];
end
```

Figure 40: Matlab code corresponding to the function **CreateTransformationMatrix**

Finally, after transforming the Reduced Sorted Hamiltonian and the boundary operators needed to create the H_{BS} of the next iteration, we saved the information of the particle numbers of this truncated basis in **CreateNewBlockBasis**. At this point we let the transformed Hamiltonian and boundary operators to be the new Block system Hamiltonian and block boundary operators of the next iteration. In Fig. 41 the sketch of the main file of the Matlab code of the NRG algorithm just described.

```
function [EnergyList] = NRGMain(U)

LatticeLength=8;
BlockBasis = CreateBasis(MinPartNumb,MaxPartNumb);
SiteBasis=CreateSiteBasis(MinPartNumb,MaxPartNumb)
BlockBasisDimension=length(BlockBasis);
SiteBasisDimension= length(S);
BlockSiteNumb=length(BlockBasis{1,1});
IterationsNumb=TotalNumbLatticeSites-BlockSiteNumb;
BlockSubSpacePartNumber=[1 2 3 4 5 6 7 8 9];
Transformations = CreateTransformationsList(LatticeLength, IterationsNumb,MaxPartNumb,MinPartNumb);
%Creation of Annihilator Matrices and Creator Matrices for the Block System
%of iteration 1.
[BlockAnnihilatorMatrices,BlockCreatorMatrices]=CreateCreatorAnnihilatorMatrices(BlockBasis);
%Creation of Annihilator Matrices and Creator Matrices for the Site System
%of iteration 1.
[SiteAnnihilatorMatrices,SiteCreatorMatrices]=CreateCreatorAnnihilatorMatrices(S);
%Creation of Block and Site Hamiltonians.
BlockHamiltonMatrix=CreateHamiltonMatrix(BlockBasis,BlockCreatorMatrices,BlockAnnihilatorMatrices,U);
SiteHamiltonMatrix= CreateHamiltonMatrix(S,SiteCreatorMatrices,SiteAnnihilatorMatrices,U);
%Start constructing the interaction term.
BlockBoundaryCreator=BlockCreatorMatrices{1,length(BlockCreatorMatrices)};
SiteBoundaryCreator= SiteCreatorMatrices{1,1};
```

```
% Since the site operator is not going to change during the whole NRG
% process we can make the change to the Full Super Basis, outside the loopr
% of iterations
SuperSiteBoundaryCreator=SiteOperatorInFullBasis(SiteBoundaryCreator,BlockBasisDimension,
                                                 SiteBasisDimension);
SuperSiteBoundaryAnnihilator=transpose(SuperSiteBoundaryCreator);
SuperSiteHamiltonMatrix = SiteOperatorInFullBasis(SiteHamiltonMatrix,BlockBasisDimension,
                                                  SiteBasisDimension);

%Erase no longer needed variables from the memory.
clear BlockCreatorMatrices
clear SiteCreatorMatrices
clear BlockAnnihilatorMatrices
clear SiteAnnihilatorMatrices

EnergyList=cell(1,IterationsNumb);
for IterationLoop=1:IterationsNumb,
SuperBlockBoundaryCreator=BlockOperatorInFullBasis(BlockBoundaryCreator,BlockBasisDimension,
                                                   SiteBasisDimension);
SuperBlockHamiltonMatrix= BlockOperatorInFullBasis(BlockHamiltonMatrix,BlockBasisDimension,
                                                   SiteBasisDimension);
SuperBlockBoundaryAnnihilator=transpose(SuperBlockBoundaryCreator);
%Creation of the FullSuperBasis that is made from the tensor product of the Block
%Basis and the Site Basis. Reduced Basis is the Basis where only the vectors with the particle's
%number that are in between the range wanted are taken.
[FullSuperBasis ReducedBasis]=CreateSuperBasis(BlockBasis,S,Transformations,IterationLoop,
                                               IterationsNumb);
ReducedBasisDim= length(ReducedBasis);
```

```
% Creates the Hamilton Matrix of the system with the new particle in the
% FullSuperBasis
SuperHamiltonMatrix=CreateSuperHamiltonMatrix(SuperBlockHamiltonMatrix,SuperSiteHamiltonMatrix,
                                              SuperBlockBoundaryCreator,SuperBlockBoundaryAnnihilator,
                                                SuperSiteBoundaryCreator,SuperSiteBoundaryAnnihilator,J);

SuperHamiltonMatrix= OperatorInReducedBasis(SuperHamiltonMatrix, FullSuperBasis, IterationLoop,
                                                                  Transformations,IterationsNumb);

SuperBlockBoundaryCreator=OperatorInReducedBasis(SuperBlockBoundaryCreator, FullSuperBasis, IterationLoop,
                                                                  Transformations,IterationsNumb);
[PositionList SortMatrix SubSpacePartNumber]=CreatePositionsListAndSortMatrix(ReducedBasis,IterationLoop,
                                                                  Transformations,IterationsNumb);
SortetSuperHamiltonMatrix= transpose(SortMatrix)*SuperHamiltonMatrix*SortMatrix;
SortetBlockBoundaryCreator= transpose(SortMatrix)*SuperBlockBoundaryCreator*SortMatrix;
SuperHamiltonEigenSystem=CreateSortetHamiltonEigenSystems(SubSpacePartNumber,SortetSuperHamiltonMatrix);
TransformationMatrix = CreateTransformationMatrix(SuperHamiltonEigenSystem,ReducedBasisDim,BlockBasisDimension,
                                                  BlockSubSpacePartNumber,SubSpacePartNumber);
BlockHamiltonMatrix = transpose(TransformationMatrix)*SortetSuperHamiltonMatrix*TransformationMatrix;
BlockBoundaryCreator= transpose(TransformationMatrix)*SortetBlockBoundaryCreator*TransformationMatrix;
BlockBasis=CreateNewBlockBasis(Transformations,IterationLoop, IterationsNumb, BlockSubSpacePartNumber,BlockBasis);
EnergyList = CreateEnergyList(BlockSiteNumb,IterationLoop,BlockBasis,BlockHamiltonMatrix,EnergyList);
clear SuperBlockBoundaryCreator;
clear SuperHamiltonMatrix;
clear SortetSuperHamiltonMatrix;
clear SortetBlockBoundaryCreator;
clear SubSpacePartNumber;
clear SuperHamiltonEigenSystem;
end
```

Figure 41: Sketch of the main file of the Matlab code

A.2 EXACT DIAGONALIZATION OF THE BOSE HUBBARD MODEL

In this section we give a brief explanation of the algorithm used to obtain the exact numerical solution of the fundamental eigenstate for the Bose Hubbard model. It might be thought that calculating the exact solution to the problem is just a topic of expressing the Hamiltonian in a certain basis and then use the diagonalization function, however from Table 1 we observe how fast the Hilbert space grows and why we must have to apply good strategies to approach the problem so that we can make it computationally treatable. In order to create the whole basis set for a fixed total particle number $N = \sum_{i=1}^{I} n_i$ in the occupation number representation $|n_1, n_2, ...n_I\rangle$, a direct way to do it computationally is shown in Fig. 42.

```
s=0;
for n1=0:N
    for n2=0:N-n1
       for n3=0:N-n1-n2
          Basis(s,:)=[n1 n2 n3 (N-n1-n2-n3)];
          s=s+1;
       end
    end
end
```

Figure 42: Standard algorithm to create the occupation number basis for $N = I = 4$

This approach, has two disadvantages: First, since the number of loops depends on the length of the lattice, the code is inflexible. Second: Since the number of loops needed is proportional to the lattice size, a Matlab programming tool will low it's efficiency considerably when the number of sites is increased.

Here, we describe a way suggested in [34] to overcome these difficulties. The idea is to give an order to the set of basis vectors expressed in the occupational number representation with fix N. Let $|n_1, n_2, ...n_I\rangle$ and $|\bar{n}_1, \bar{n}_2, ...\bar{n}_I\rangle$ be two different basis vectors, there must exists an index k, with $1 \leqslant k \leqslant I-1$ such that $n_i = \bar{n}_i$ for $1 \leqslant i \leqslant k-1$ and $n_k \neq \bar{n}_k$. Notice that if $k = I$, then the vectors must be equal because of the condition of having fixed N. We say $|n_1, n_2, ...n_I\rangle > (<)|\bar{n}_1, \bar{n}_2, ...\bar{n}_I\rangle$ if $n_k > (<)\bar{n}_k$. It is easy to see that according to this order structure $|N, 0, ..., 0\rangle$ is the greatest vector in the set and $|0, ..., N\rangle$ is the smallest one.

Now, lets examine the way to generate all the basis vectors in descending order starting from $|N, 0, ..., 0\rangle$. Assume the last vector you create is $|n_1, n_2, ...n_I\rangle$, then the next inferior vector is constructed using the following receipt:

Take the $n_j \neq 0$ such that $n_i = 0$ for all $j+1 \leqslant i \leqslant I-1$, then the next basis vector is $|\bar{n}_1, \bar{n}_2, ...\bar{n}_I\rangle$ with:

- $\bar{n}_i = n_i$ for $1 \leqslant i \leqslant j-1$;
- $\bar{n}_j = n_j - 1$;
- $\bar{n}_{j+1} = N - \sum_{i=1}^{j} \bar{n}_i$;
- $\bar{n}_i = 0$ for $i \geqslant j+2$;

The procedure ends with the lowest vector $|0, ..., N\rangle$ as expected. This code is flexible and therefore does not depend on the number of particle or lattice size, in our opinion the way of solving the difficulties mentioned before by [34] is very creative and useful. We give in Fig 43 an example of how to implement the algorithm in Matlab.

```
%Creating a Basis in the Occupational Number representation. Where there
%are N particles and the number of latice sites is M.
function [BasisVect] = CreateBasisExact(M,N)
%Dimension of the Basis.
D= factorial(N+M-1)/(factorial(N)* factorial(M-1));
BasisVect(1,:)=zeros(1,M);
BasisVect(1,1)=N;
for  l= 2:D,
    s=0;
    sum=0;
    for j= M-1:-1:1,
          if BasisVect(l-1,j)~=0 && s==0
           s=1;
           for i=1:j-1, % Values before k are the same as the former inmediatly smaller vector.
                 BasisVect(l,i)=BasisVect(l-1,i);
                 sum= sum+BasisVect(l,i);
           end
           BasisVect(l,j)= BasisVect(l-1,j)-1;
           sum=sum+BasisVect(l,j);
           BasisVect(l,j+1)= N-sum;
           for t= j+2:M,
               BasisVect(l,t)=0;
           end
          end
    end
end
```

Figure 43: Matlab code to the flexible algorithm for creating the Basis of a Bose Hubbard model with fixed N

In Table 2 an example of the order basis generated by this code for $N = I = 3$.

n_1	n_2	n_3
3	0	0
2	1	0
2	0	1
1	2	0
1	1	1
1	0	2
0	3	0
0	2	2
0	1	2
0	0	3

Table 2: Basis generated with the algorithm described above for $N = I = 3$

With the basis formed we can proceed to create the Hamiltonian matrix. Notice that there are two parts in the Hamiltonian, the kinetic one H_{kin} which will contribute to the non-diagonal terms and the interacting one H_{int} which is diagonal in our basis of occupational number representation since it is composed of particle's

number operators. The naive method to proceed would be to calculate the corresponding D^2 elements $\langle u|H|v\rangle$ one by one, with D the number of basis vectors. As we have seen D is usually a big number, for $N = I = 11$, $D = 352716$ and most of these matrix elements will vanish, thus the matrix can be store in a sparse form. Here, we follow again the idea given in [34], in which we evaluate the term $a_i^\dagger a_j$ which sends one basis vector to another, and the problem is to seek the position in the basis array list of this last vector. Hence, instead of calculating every matrix element we only calculate those that are non-vanishing.

This task of comparing a vector with all the vectors in a list is simplified very much if we invoke the so called hashing technique. The main idea to create a tag function in such a way that every vector in the list is identified by a unique tag. In our code we use the following: $T(v) = \sum_{i=1}^{I} \sqrt{p_i} v_i$ with $p_i = 100 * i + 3$ and v_i the ith component of v; it is easy to see that $T(v)$ is different for every vector in the basis set. Therefore, with this technique, to see whether two vectors are the same, rather than comparing their elements one by one we only need to compare their tags which is computationally more efficient. Now, the main problem has been reduced to search a number inside an unsorted array representing the tags of each vector basis. We used the Newton binary method to develop this task.

The Newton binary method organizes the list of numbers in ascending order, and starts asking whether the element under consideration is equal, greater or smaller than the element located in the middle of the list. Hence, if the element matches that in the middle point, the task is done; if the element is smaller or greater the algorithm keeps searching only in one or the other half of the chain and so on. Since the list is finite the element will match the middle point number of the correspondent list at a certain step. The implementation of the Newton binary method in our code reduced the time of compilation approximately in a ratio of $1 : 20$ for the case of $N = I = 8$

Finally, once the matrix Hamiltonian is constructed in a sparse form, we can proceed to diagonalize it. Usually, we are only interested in the fundamental and first exited states; when this is the case it is possible to use the [14] Lanczos algorithm to compute them. The eigenvalues and eigenvectors converges as the iteration goes on, specially the extremal eigenvalues are the first to converge. In Matlab the function **eigs** is based on the Lanczos algorithm and we have used it to find the ground state of the Hubbard Bose model.

$$[Evec Eval] = eigs(H, 2, 'sa')$$

This command returns the two smallest eigenvalues $Eval$ in a 2×2 matrix and their corresponding eigenvectors $Evec$ in a $D \times 2$ matrix.

We have explained up to a certain detail the Matlab codes that we used to produce the results for comparing the ground states of the Bose Hubbard model by using the NRG method and the exact diagonalization.

A.3 DMRG ALGORITHM FOR HEISENBERG MODEL

In this section we present a sketch of the Matlab code implemented for the DMRG algorithm in the case of the Heisenberg model. The code is developed very much as is explain in chapter 3.

We treat the environment block separately meaning that we develop a renormalization procedure for left and right sides at the same time. When the Hamiltonian presents reflection symmetry [23], it is possible to consider system and environment to be identical.

Once we have constructed the Hamiltonian operators for the two-site left and right blocks, we construct the respective enlarge blocks by taking the tensor product of the block operators with the identity of the one site Hilbert space. We do this procedure through the functions **CreateRightOperatorInFullBasis** and **CreateLeftOperatorInFullBasis**, for both, left and right sides as is shown in Fig 44.

```
%We start this cycle after defining a left and right systems of two sites.

for iteration=1:MaxIteration
%Create Interacting Term of left system Block-Site. We use Middle Basis for the enlarged system.
%Express Left block-Site Hamiltonian in terms of the Enlarged tensor product  Basis.
HLeftBlockMiddle=sparse(CreateLeftOperatorInFullBasis(HamiltonianLeftBlock,2));
%Sig_zLast correspond to the sigma-z right boundaryoperator of the left block
Sig_zLastMiddle=sparse(CreateLeftOperatorInFullBasis(Sig_zLast,2));
Sig_plusLastMiddle=sparse(CreateLeftOperatorInFullBasis(Sig_plusLast,2));
[Dim Dimm]=size(HamiltonianLeftBlock);
%Expresses the adding site in terms of the enlarged basis.
Sig_zSiteMiddle=  CreateRightOperatorInFullBasis(Sig_zSite,Dim);
Sig_plusSiteMiddle=  CreateRightOperatorInFullBasis(Sig_plusSite,Dim);
%Left enlarged Hamiltonian.
HamiltonianLeftBlock_Site=HLeftBlockMiddle-J*(Sig_zLastMiddle*Sig_zSiteMiddle+
      (Sig_plusLastMiddle*ctranspose(Sig_plusSiteMiddle)+ ctranspose(Sig_plusLastMiddle)*Sig_plusSiteMiddle)/2);
%Express Right Block-Site system in terms of the new enlarged Basis.
HRightBlockMiddle=sparse(CreateRightOperatorInFullBasis(HamiltonianRightBlock,2));
Sig_zRSiteMiddle=CreateLeftOperatorInFullBasis(Sig_zSite,Dim);
Sig_plusRSiteMiddle= CreateLeftOperatorInFullBasis(Sig_plusSite,Dim);
%Expresses the adding site in terms of the right enlarged basis.
Sig_zRFirstMiddle=sparse(CreateRightOperatorInFullBasis(Sig_zRFirst,2));
Sig_plusRFirstMiddle=sparse(CreateRightOperatorInFullBasis(Sig_plusRFirst,2));
%Right enlarged Hamiltonian.
HamiltonianRightBlock_Site=HRightBlockMiddle-J*(Sig_zRSiteMiddle*Sig_zRFirstMiddle+
  (Sig_plusRSiteMiddle*ctranspose(Sig_plusRFirstMiddle)+ctranspose(Sig_plusRSiteMiddle)*Sig_plusRFirstMiddle)/2);
```

Figure 44: First part of the iteration loop of the DMRG Matlab code.

Then we proceed to construct the super Hamiltonian composing the left and right enlarged blocks. We must express all the operators in the super basis which is the tensor product of the basis of both sides. Finally we develop the renormalization procedure, as can be seen in Fig 45. We are going to explain a few things about the function **CreatePartialDensityMatrix** that we use to construct the reduced density matrix of the left enlarged block.

```
%Hamiltonian of the Super System.
[SDim SDim]=size(HLeftBlockMiddle);
%Expressing all the operators in terms of the new super basis.
HLeftBlockSuper=CreateLeftOperatorInFullBasis(HamiltonianLeftBlock_Site,SDim);
Sig_zSiteSuper=  CreateLeftOperatorInFullBasis(Sig_zSiteMiddle,SDim);
Sig_plusSiteSuper=  CreateLeftOperatorInFullBasis(Sig_plusSiteMiddle,SDim);
HRightBlockSuper=CreateRightOperatorInFullBasis(HamiltonianRightBlock_Site,SDim);
Sig_zRSiteSuper=CreateRightOperatorInFullBasis(Sig_zRSiteMiddle,SDim);
Sig_plusRSiteSuper= CreateRightOperatorInFullBasis(Sig_plusRSiteMiddle,SDim);
%Total Hamiltonian
HtotalSuper=HLeftBlockSuper+HRightBlockSuper-J*(Sig_zSiteSuper*Sig_zRSiteSuper
   +(Sig_plusSiteSuper*ctranspose(Sig_plusRSiteSuper)+ctranspose(Sig_plusSiteSuper)*Sig_plusRSiteSuper )/2);
%Renormalization procedure:Superblock ground state
[GGroundState GGroundEnergy]=GroundStateSuperBlock1(HtotalSuper);
Ground(iteration,1)=GGroundEnergy/(((iteration+1)*2)+2);
%Creation of the left and right Reduced Density Matrices
[PartialDensityMatrix]=CreatePartialDensityMatrix(GGroundState);
[RPartialDensityMatrix]=CreateRightPartialDensityMatrix(GGroundState);
%Diagonalization of the Reduced Density Matrices. Creation of the
%tranformation Matrices
[EigenVectors EigenValues]=DensityMatrixDiagonalization(PartialDensityMatrix,m);
[REigenVectors REigenValues]=DensityMatrixDiagonalization(RPartialDensityMatrix,m);
%Projecting on the truncated set of eigenbasis.
HamiltonianLeftBlock=ctranspose(EigenVectors)* HamiltonianLeftBlock_Site * EigenVectors;
HamiltonianRightBlock=ctranspose(REigenVectors)* HamiltonianRightBlock_Site * REigenVectors;
%For the next iteration we also need to express Sig_zFirst in terms of the
%Left Block-Site Basis.
Sig_zLast=ctranspose(EigenVectors)*Sig_zSiteMiddle* EigenVectors;
Sig_plusLast=ctranspose(EigenVectors)*Sig_plusSiteMiddle* EigenVectors;
%Left Block-Site Basis.
Sig_zRFirst=ctranspose(REigenVectors)* Sig_zRSiteMiddle * REigenVectors;
Sig_plusRFirst=ctranspose(REigenVectors)* Sig_plusRSiteMiddle * REigenVectors;
end
```

Figure 45: Second part of the iteration loop of the DMRG Matlab code.

Since from the second iteration of the algorithm we lose all the information about the basis vectors themselves, we have to keep in mind at least the order of the basis vectors in which the fundamental ground state is expressed. The ground state is express in the tensor product of the left and right enlarged basis, this means that it has the form $|\psi\rangle = \sum_{i_1,i_2} \psi_{i_1,i_2}|i_1\rangle|i_2\rangle$. Furthermore the order is given as in Fig 46:

$$
\begin{aligned}
|\psi\rangle = &\psi_{1,1}|1,1\rangle + \psi_{1,2}|1,2\rangle + \ldots + \psi_{1,N_E}|1,N_E\rangle \\
&\psi_{2,1}|2,1\rangle + \psi_{2,2}|2,2\rangle + \ldots + \psi_{2,N_E}|2,N_E\rangle \\
&\vdots \\
&\psi_{N_S,1}|N_S,1\rangle + \psi_{N_S,2}|N_S,2\rangle + \ldots + \psi_{N_S,N_E}|N_S,N_E\rangle,
\end{aligned}
$$

Figure 46: Ground state expressed in the tensor product basis. The matrix elements are calculated by summing up products of elements marked with the same color.

this structure is useful when calculating the reduced density matrix, given by $\rho_S = \sum_{i_1', i_1} (\sum_{i_2} \psi_{i_1,i_2} \psi^*_{i_1',i_2}) |i_1\rangle\langle i_1'|$, because it's matrix elements are calculated by summing up the product of two parallel elements chosen from two rows whose location determines the matrix element under study. In Fig 46 the elements marked with the same color are to be multiplied in order to calculate the matrix elements $\rho_{2,N_S} = \rho^*_{N_S,2}$.

The rest of the code of the renormalization procedure is more or less expected from the explanation given in chapter 3.

BIBLIOGRAPHY

[1] Taipei. Density Matrix Renormalization Group. Winter school. https://sites.google.com/site/dmrg101/melko. Accessed: 2013-04-28.

[2] A. P. Balachandran, T. R. Govindarajan, Amilcar R. de Queiroz, and A. F. Reyes-Lega. Entanglement and particle identity: A unifying approach. *Phys. Rev. Lett*, 110:080503, February 2013.

[3] George .G Batrouni and R.T Scalettar. *Quantum Phase Transitions*. OXFORD, University Press.

[4] Sven Binder. *The Numerical Renormalization Group applied to the Bose Hubbard Model*. 1 edition, 2007.

[5] Ming-Chiang Chung and Ingo Peschel. Density-matrix spectra for two-dimensional quantum systems. *Phys. Rev. B*, 62:4191–4193, August 2000.

[6] Hugo Alejandro Contreras. *Quantum Phase Transitions,Berry Phase and Chern Numbers*. Master Thesis, 2008.

[7] Ernest. R Davidson. The iterative calculation of a few of the lowest eigenvalues and corresponding eigenvectors of large real-symmetric matrices. *J.Comput. Phys*, 17:87–94, January 1975.

[8] Gabriele. De Chiara, Matteo. Rizzi, Davide. Rossini, and Simone. Montangero. Density Matrix Renormalization Group for dummies. *eprint arXiv:cond-mat/0603842*, March 2006.

[9] Gabriele De Chiara, Luca Lepori, Maciej Lewenstein, and Anna Sanpera. Entanglement spectrum, critical exponents, and order parameters in quantum spin chains. *Phys. Rev. Lett*, 109:237208–237213, December 2012.

[10] Amit Dutta, Uma Divakaran, Diptiman Sen, Bikas Chakrabarti, Thomas Rosenbaum, and Gabriel Aeppli. Quantum Phase Transition in a transverse field spin models: From Statistical Physics to Quantum Infomation. *eprint arXiv:1012.0653*, November 2012.

[11] F Franchini, A. R Its, B. Q Jin, and V.E Korepin. Ellipses of constant entropy in the xy spin chain. *J. Phys. A*, 40:8467–8478, July 2007.

[12] Um Jaegon, Sung-Ik Lee, and Beom Jun Kim. Quantum Phase Transitions and Finite Size Scaling of the one-Dimensional Ising model. *J. Kor. Phys.Soc*, 50(1): 285–289, January 2007.

[13] Dragi Karevski. Surface and bulk critical behaviour of the xy chain in a transverse field. *J. Phys. A*, 33:L313–L317, May 2000.

[14] C Lanczos. An iteration method for the solution of the eigenvalue problem of linear differential and integral operations. *J.Res. Natl Bur. Stand*, 45(4):258–282, October 1950.

[15] N.P Landsman. *Lecture notes on Quantum Phase Transitions*. 2012.

[16] Jose I Latorre, Enrique Rico, and Vidal Guifre. Ground state entanglement in quantum spin chains. *eprint arXiv:quant-ph/0304098*, 47, April 2008.

[17] Michel Le Bellac, Fabrice Mortessagne, and George. G Batrouni. *Equilibrium and Non-Equilibrium Statistical Thermodynamics*. Cambridge, University Press.

[18] Elliott Lieb, Theodore Schultz, and Daniel Mattis. Two Soluble Models of an Antiferromagnetic Chain. *Ann.Phys*, 16:407–466, 1961.

[19] Michael A. Nielsen and Chuang Isaac L. *Quantum Computation and Quantum Information*. Cambridge University Press, 1st edition, 2000.

[20] Ingo Peschel and Viktor Eisler. Reduced density matrices and entanglement entropy in free lattice models. *J. Phys. A*, 42(50), December 2009.

[21] Matteo Rizzi, Davide Rossini, Simone De Chiara, Gabriele Montangero, and Rosario Fazio. Phase diagram of spin-1 bosons on one-dimensional lattices. *Phys. Rev. Lett*, 95(240404), December 2005.

[22] Subir Sachdev. *Quantum Phase Transitions*. Cambridge University Press, 2nd edition, 2011.

[23] Ulrich Schollwock. The Density Matrix Renormalization Group. *Rev.Mod.Phys*, 77, April 2005.

[24] Franco Strocchi. *Lecture Notes in Physics: Symmetry Breaking*. Springer, 2nd edition, 2008.

[25] Masuo Suzuki. Static and Dynamic Finite Size Scaling Theory based on the Renormalization Group approach. *Prog. Theor.Phys*, 58(4):1142–1149, October 1977.

[26] Malte. C Tichy, Florian Mintert, and Andreas Buchleitner. Essential entanglement for atomic and molecular physics. *J. Phys. B*, 44(19), September 2011.

[27] Steven. R White. Density matrix formulation for Quantum Renormalization Groups. *Phys. Rev. Lett*, 69(19):2863–2866, May 1992.

[28] Steven. R White. Density Matrix algorithms for Quantum Renormalization Groups. *Phys. Rev. B*, 48(14), January 1993.

[29] Steven. R White and David Huse. Numerical Renormalization-Group study of low-lying eigenstates of the antiferromagnetic s = 1 heisenberg chain. *Phys. Rev. B*, 48(6):3844–3852, August 1993.

[30] Steven. R White and Reinhard. M Noack. Real-Space Quantum Renormalization Groups. *Phys. Rev. Lett*, 68(24):3487–3490, June 1992.

[31] K.G. Wilson. The renormalization group: Critical phenomena and the kondo problem. *Rev. Mod. Phys.*, 47(19):773–840, October 1975.

[32] T Xiang and G.A Gehring. Numerical solution of S =1 antiferromagnetic spin chains using a truncated basis expansion. *Phys. Rev. B*, 48:303–310, July 1993.

[33] Julia. M Yeomans. *Statistical Mechanics of Phase Transitions*. Clarendon Press, Oxford.

[34] J.M Zhang and R.X Dong. Exact diagonalization: the Bose Hubbard model as an example. *Eur. J. Phys.*, 31:591–602, April 2010.

[35] Shi-Liang Zhu. Scaling of Geometric Phases close to the Quantum Phase Transition in the xy spin chain. *Phys. Rev. Lett*, 96(077206), February 2006.